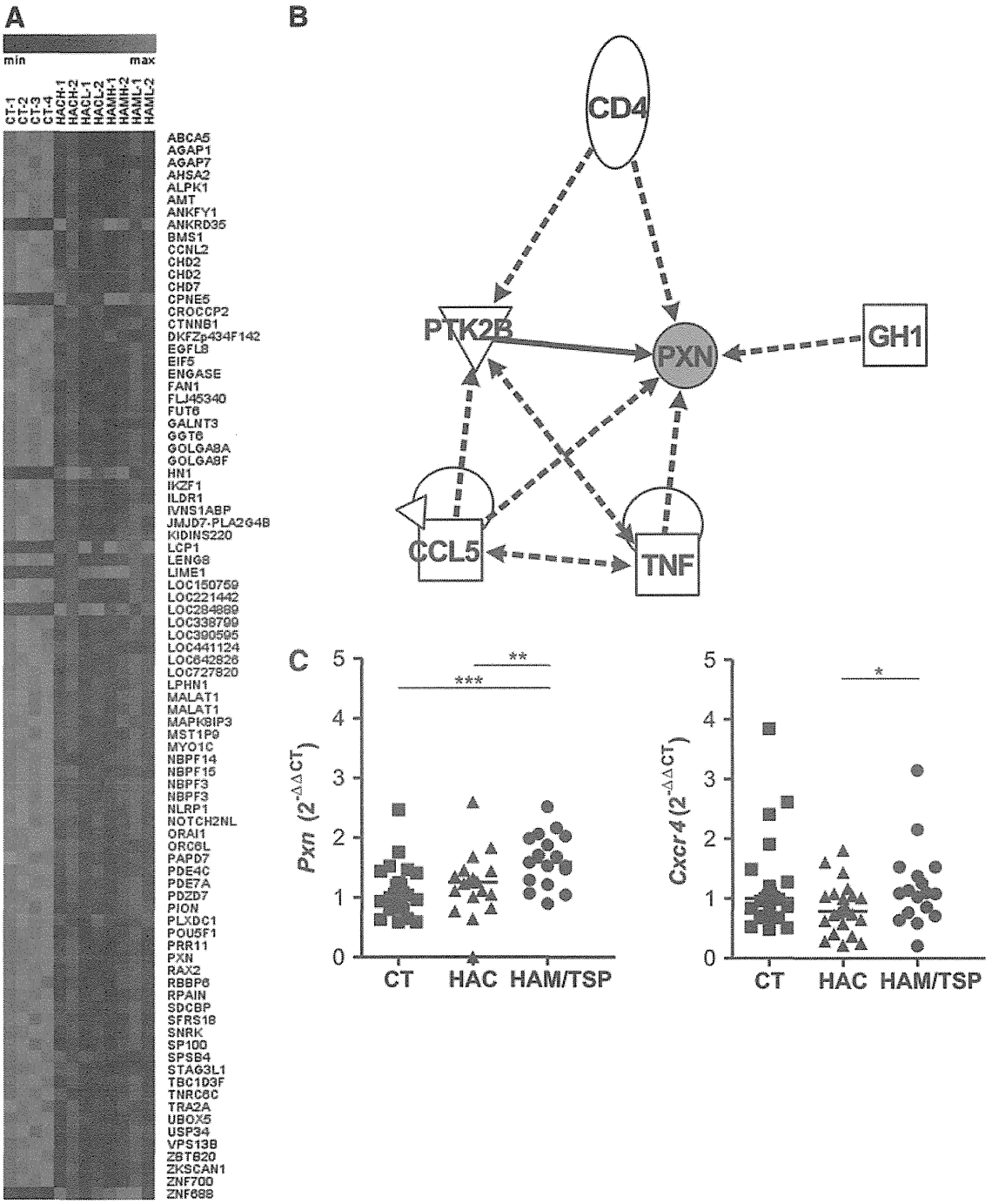

FIG. 3. Expression profiling of genes differentially expressed in HTLV-1. **(A)** Gene expression heat map of analyses of 84 differently expressed genes between the CT vs. HAC and the CT vs. HAM/TSP groups. **(B)** Schematic of molecular interactions. The network image was created using IPA software. The lines represent regulation of function between two genes. **(C)** Real-time PCR of *Pxn* and *Cxcr4* mRNA in $CD4^+$ T cells from CT, HAC, and HAM/TSP. The Mann–Whitney *U*-test was used to evaluate differences among groups (*$p \leq 0.05$; **$p \leq 0.01$; ***$p \leq 0.001$). CT, healthy control; HAC, asymptomatic HTLV-1 carrier; HAM/TSP, HTLV-1-associated myelopathy/tropical spastic paraparesis.

correlated in HTLV-1-infected groups, being higher in the HAM/TSP group. This observation reinforced the fact that these cells may contribute to the progression of HTLV-1-related diseases.[25,33] Although several authors have published TAX expression and PVL quantification values in HTLV-1-infected individuals, the standard reference values for these parameters have not been well established yet. In our study, we measured the levels of TAX expression and by setting the median value we defined low and high TAX expression samples. Hierarchical clustering analysis showed that CT and HTLV-1-infected groups clustered separately. Here, we also show that $CD4^+$ T cells from HAC and HAM/TSP samples clustered separately regardless of TAX expression. Thus, our results demonstrate that genes are differentially expressed according to individuals' HTLV clinical status in $CD4^+$ T cells. However, it would be important to analyze

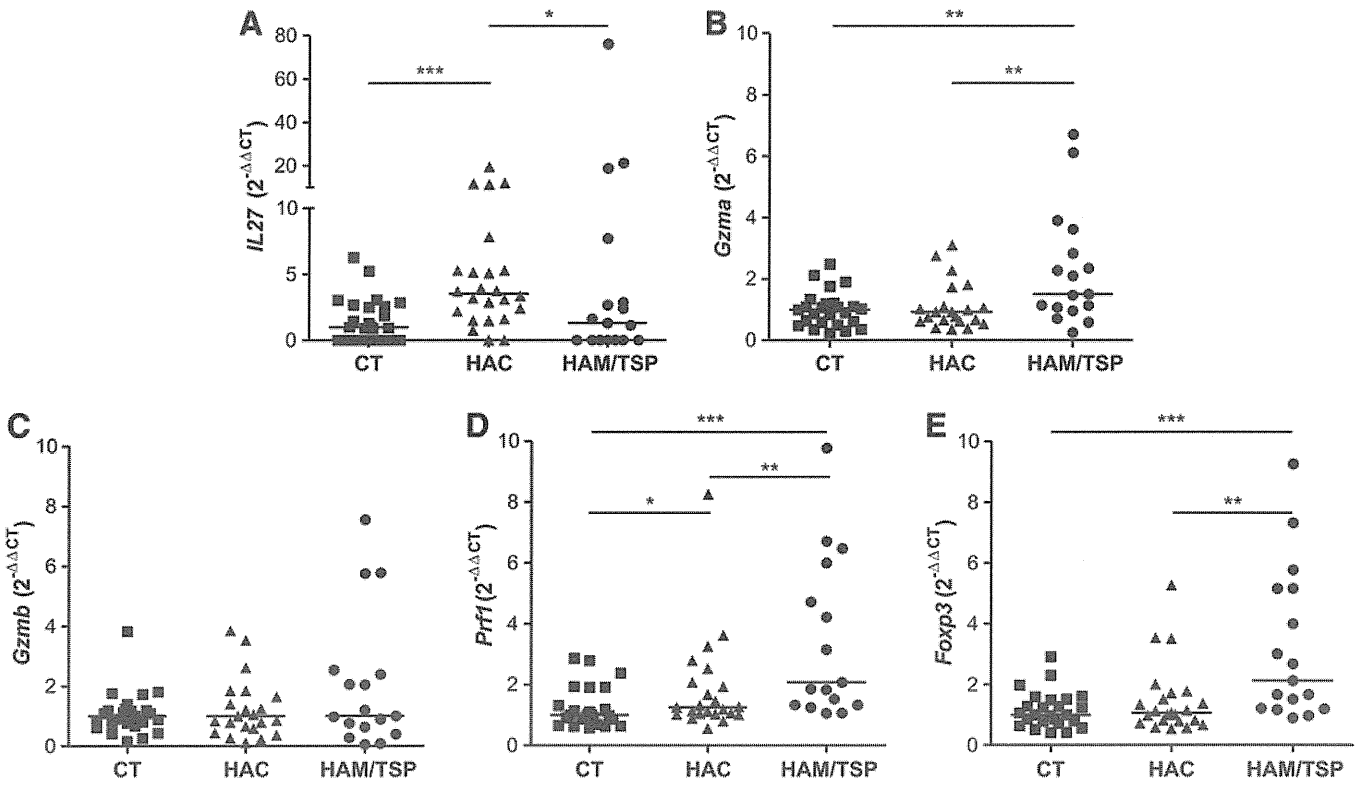

FIG. 4. *IL27*, *Gzma*, *Gzmb*, *Prf1*, and *Foxp3* gene expression by real-time PCR. Gene expression levels comparison of *IL27* (**A**), *Gzma* (**B**), *Gzmb* (**C**), *Prf1* (**D**), and *Foxp3* (**E**) among the CT, HAC, and HAM/TSP groups. The Mann–Whitney *U*-test was used to evaluate differences among groups (*$p \leq 0.05$; **$p \leq 0.01$; ***$p \leq 0.001$). CT, healthy control; HAC, asymptomatic HTLV-1 carrier; HAM/TSP, HTLV-1-associated myelopathy/tropical spastic paraparesis.

gene expression between the HAC and HAM/TSP groups with similar levels of TAX expression and PVL.

It was reported that the global gene expression profile did not allow observation of two independent clusters for HAC and HAM/TSP; however, ATLL samples were suitably clustered independently.[38] Another previous study did not find differences between the HAC and HAM/TSP groups when clustering $CD4^+$ T cells.[37] These findings could be explained by how the sampling was done. In our analysis, individual samples were submitted to microarray analysis.

We analyzed *Pxn* and *Cxcr4* gene expression since they are involved in cell migration. In response to its binding ligand stromal cell-derived factor-1 (SDF-1), CXCR4 induces downstream signaling by several different pathways. SDF-1 binding to CXCR4 promotes actin polymerization to initiate cell motility. CXCR4 triggers the activation of the src family of protein tyrosine kinases and then the focal adhesion complexes such as RAFTK/Pyk2, focal adhesion kinase, Crk, and paxillin are phosphorylated and activated.[39–41] The focal adhesion components paxillin and Crk play a critical role in the chemotactic signaling pathways.[42]

Although the *Cxcr4* gene did not show deregulation in microarray analysis, the *Pxn* gene is a member of the *Cxcr4* pathway. The *Pxn* gene was overexpressed in the CT group compared to the HTLV-1-infected group in microarray analysis. Intriguingly, after a validation process this gene was significantly up-regulated in the HTLV-1-infected group (HAC+ HAM/TSP). The discordant results between microarray and qPCR techniques are explained by the inherent pitfalls of each technique.[43–47] To confirm the gene expression results obtained from microarray analysis qPCR is frequently used as a validation tool. Furthermore, many different platforms exist for both microarray and qPCR analyses that have led to debates over which techniques produce the most exact measurements of gene expression.[48–50] Additionally, we can also explain our discrepant results based on the fact that microarray and qPCR were not performed with the same number of samples.

CXCR4 is highly expressed by leukocytes in the immune and central nervous systems.[51,52] In this study, *Cxcr4* gene expression was up-regulated in the HAM/TSP group compared to the HAC group and no difference in CXCR4 protein levels by flow cytometry was observed among the studied groups. These different results between *Cxcr4* mRNA and protein expression can be explained by the fact that there are posttranscriptional mechanisms that might control the translation of the protein. The presence of this posttranscriptional control is demonstrated in many studies, suggesting that there is a poor correlation between the mRNA and protein pools in eukaryotic cells.[53–58]

On the other hand, one previous study demonstrated that CXCR4 levels in HTLV-1-infected cell lines were lower than in noninfected cell lines.[59] This could be explained by the type of cell samples used, since we are working with cells belonging to HTLV-1-infected individuals, in which genetic susceptibility should be taken into account. It was also demonstrated that the inhibition of the SDF-1α-CXCR4 axis by the CXCR4 antagonist AMD3100 suppresses the migration of cultured cells from ATL patients and murine lymphoblastoid cells from HTLV-1 TAX transgenic mice. Therefore, these results show the association of the SDF-1alpha/CXCR4 interaction as

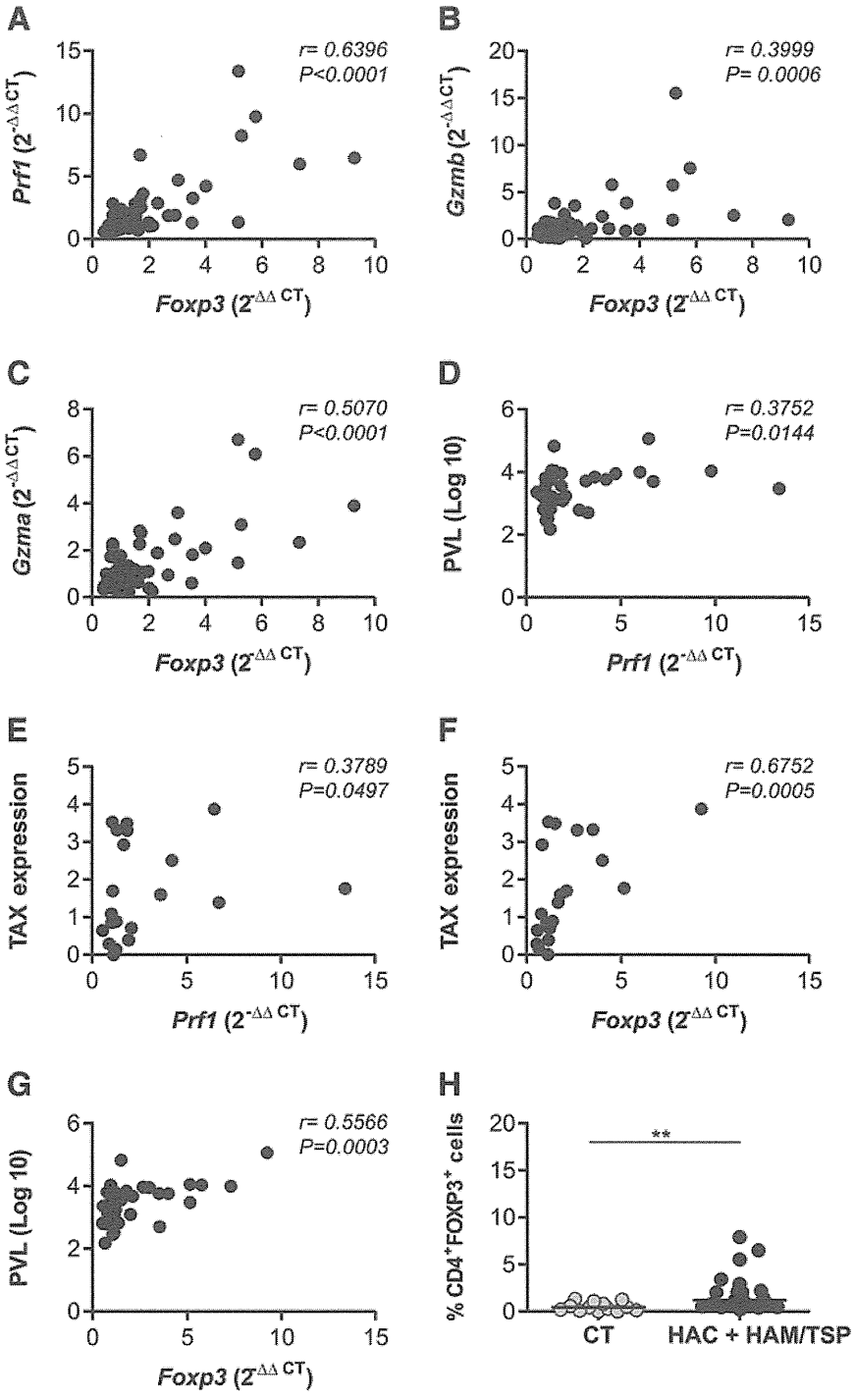

FIG. 5. Correlation between cell lysis-related genes and *Foxp3* in $CD4^+$ T cells, percentage of TAX expression, and proviral load in peripheral blood mononuclear cells (PBMCs). The *Foxp3* expression in $CD4^+$ T cells positively correlated with *Prf1* **(A)**, *Gzmb* **(B)**, and *Gzma* **(C)** expression. A positive correlation between PVL and *Prf1* **(D)**, TAX expression and *Prf1* **(E)**, TAX expression and *Foxp3* **(F)**, and PVL and *Foxp3* **(G)** was observed. The correlation was calculated by the Spearman method. **(H)** The percentage of FOXP3-expressing cells in the $CD4^+$ population from PBMCs. The Mann–Whitney *U*-test was used to evaluate differences among groups (**$p \leq 0.01$). CT, healthy control; HAC, asymptomatic HTLV-1 carrier; HAM/TSP, HTLV-1-associated myelopathy/tropical spastic paraparesis; PVL, proviral load.

one mechanism of leukemic cell migration and this may offer a new target as part of combination therapy for ATLL.[60]

HTLV-1-infected lymphocytes may cross the blood–brain barrier and may generate an intensive immune response leading to the development of HAM/TSP. All the aforementioned findings lead us to believe that there is a dynamic regulation of *Cxcr4* expression, since the *Pxn* and *Cxcr4* genes are overexpressed in the HAM/TSP group. This result suggests that this pathway could be deregulated in these patients and could lead to $CD4^+$ T cell migration to the CNS. This way, our data suggest that the *Pxn* and *Cxcr4* genes may be acting together in $CD4^+$ T cells.

We observed that the *IL27* gene was up-regulated in the HAC group when compared to the CT and HAM/TSP groups. IL-27 is a member of the IL-12 cytokine family and has many functions in immune response such as induction of proliferation of naive specificity and also as an early product of activated antigen-presenting cells.[61] Moreover, it has been shown that IL-27 is capable of regulating T helper subpopulations (Th1, Th2, and Th17) during acute and chronic infection and inflammatory processes.[62–66] Previous studies have reported that IL-27 inhibits HIV-1 replication in T cells and macrophages and HCV replication.[67–70] Furthermore, IL-27 may play an antiviral and antitumor role in ATLL and other

lymphoid malignancies[71] and it has gathered considerable attention in terms of its therapeutic application in immune disease. This way, IL-27 was shown to suppress experimental autoimmune encephalomyelitis during bone marrow stromal cell treatment.[72] Other studies reported suppression of experimental autoimmune uveoretinitis (EAU),[73] inflammation in the joint, and severe arthritis by administration of IL-27. In addition, IL-27 administered *in vivo* showed its anti-inflammatory effects on a delayed type hypersensitivity model, demonstrating its therapeutic potential against some diseases of immune origin.[74] However, IL-27 may be an effective therapeutic agent for HTLV-1-infected individuals in order to suppress the inflammation caused by retroviruses and consequently to decrease the risk of HAM/TSP development. Therefore, the specific role of this cytokine in HTLV-1 infection remains unclear.

The perforin/granzyme mechanism is mainly carried out by circulating white blood cells such as CTLs and natural killer (NK) cells. Several studies have shown that Treg cells may use the perforin/granzyme pathway as a system to suppress the function of immune cells by killing them.[31,75,76] It was demonstrated that activated murine Treg cells suppressed B cell proliferation in a granzyme B- and perforin-dependent fashion.[76] Likewise, the activated human Treg cells expressed granzyme A and/or B and could use the perforin pathway to cause autologous target cell death.[75] The transcriptional factor FOXP3 is considered one of the main specific markers for Treg cells[77] whose expression is a critical mediator for the development and the function of these cells.[78] Treg cells are major effector cells during immune response by the perforin/granzyme pathway. Considering this, we selected *Gzma*, *Gzmb*, *Prf1*, and *Foxp3* for gene expression analysis.

The level of *Prf1* and *Gzma* gene expression was significantly higher in the HAM/TSP group compared to the CT and HAC groups. No differences were observed in intracellular PRF1 among the studied groups. Protein detection and quantification are potent tools since mRNA detection could not guarantee that protein will be translated or functional. Thus there could be posttranscriptional mechanisms that regulate the expression of these molecules. Moreover, measurement of granzyme and perforin mRNA is better than immunostaining of granzyme and perforin proteins as a correlate of cytotoxicity, because the granzyme and perforin proteins do not accumulate in the cell but are rapidly and continually discharged in the lytic granules.[37] Therefore, all these considerations can explain our results.

Although it has been demonstrated that HTLV-1 has a tropism to Treg cells,[79] reduced FOXP3 protein expression in HTLV-1-infected cells of HAM/TSP patients has been reported.[80,81] However, in our analysis of *Foxp3* gene expression, we also noticed a significant increase in the HAM/TSP group compared to the CT and HAC groups. We also observed a positive correlation among *Gzma*, *Gzmb*, and *Prf1* to *Foxp3*. In addition to that, there was also a positive correlation between the *Foxp3* gene and PVL and the *Foxp3* gene and TAX expression. These data are consistent with the results from a previous report[82] describing higher $FOXP3^+$ expression in $CD4^+$ T cells of individuals with HAM/TSP compared to healthy individuals. In addition, the researchers have also observed a positive correlation between FOXP3 and PVL and FOXP3 and TAX expression. We also found an increased frequency of $CD4^+FOXP3^+$ cells in HTLV-1-infected individuals, as reported previously.[82,83] In our results, we showed that *Foxp3* gene expression levels were increased in the HAM/TSP group compared to the HAC group, while the proportions of $CD4^+FOXP3^+$ cells were higher in the HAC group compared to the HAM/TSP group. This discordance may be due to differences between both applied techniques. In general, the sensitivity of real-time RT-PCR is higher than that of flow cytometry.[84]

Many studies on solid-organ transplant recipients (heart, kidney, and intestine) have demonstrated a direct correlation between Treg marker FOXP3 and the cytotoxic T cell effector molecules (granzyme B, perforin, and granulysin) in the process of acute rejection.[85–89] Therefore, in our study we speculate that FOXP3 is correlated with the cytotoxic T cell effector molecules (*Gzma*, *Gzmb*, and *Prf1*) in HTLV-1 infection. One previous study suggested two possibilities for the role of Treg cells in HTLV-1 infection. First, $FOXP3^+$ T cells have hyperproliferation ability[90] and this could collaborate in the clonal expansion of HTLV-1-infected cells. Second, HTLV-1 can invade the immune system by direct infection of this immunosuppressive cell population. Consequently, HTLV-1 infection of $FOXP3^+$ T cells can enable the virus to increase or maintain its proviral load and thus reach a state of persistent infection.[91] With this in mind, we suggest another possibility for the role of Treg cells. Treg cells may use the perforin/granzyme pathway as a system to suppress the immune cells by killing them. This way, the increase of $FOXP3^+$ T cells analyzed in HTLV-1 infection may contribute to immunodeficiency, which is observed in HTLV-1 infection.[92]

In a previous study, we reported differentially expressed genes in $CD8^+$ T cells isolated from the same population as this study. Our results showed that patients with HAM/TSP have high expression levels of degranulation-related genes (*Gzmh* and *Prf1*) and of the cytoskeletal adaptor *Pxn*. We indicated that *Gzmb* and *Zap70* genes were overexpressed in HTLV-infected individuals compared to the healthy control group. We also found that *Ccl5* was higher in the HAM/TSP group compared to the HAC and CT groups. Therefore, our findings showed that $CD8^+$ and $CD4^+$ T cells from HAM/TSP patients have an inflammatory and active profile.[93]

In conclusion, we demonstrated that *Pxn*, *Cxcr4*, *IL27*, and *Gzma* gene expression in $CD4^+$ T cells differs between the HAC and HAM/TSP groups regardless of TAX expression. *Prf1* and *Foxp3* genes are increased in the HAM/TSP group compared to the HAC group and present a positive correlation to the expression of TAX and PVL. We believe that the *IL27*, *Pxn*, *Cxcr4*, *Gzma*, *Prf1*, and *Foxp3* genes are novel molecules that could play an important role in HTLV-1 infection. Moreover, Treg may be a future strategy for the treatment and prevention of HTLV-1-infected individuals. However, further studies are required to elucidate the molecular mechanisms of $CD4^+$ T cell involved in HTLV-1 infection.

Acknowledgments

The authors thank Rochele Azevedo for quantification of the proviral load, Patrícia Vianna Bonini Palma for flow cytometry analysis, Amelia Goes de Araujo for her assistance with the microarray technique, Maurício Cristiano Rocha Junior for help in writing the paper, and Prof. Charles Bangham

for TAX expression analysis. They are also grateful to the patients. This work was supported by Fundação Hemocentro de Ribeirão Preto (FUNDHERP) and São Paulo Research Foundation (FAPESP-Process number: 2011/21740-7)

Author Disclosure Statement

No competing financial interests exist.

References

1. Poiesz BJ, Ruscetti FW, Gazdar AF, *et al.*: Detection and isolation of type C retrovirus particles from fresh and cultured lymphocytes of a patient with cutaneous T-cell lymphoma. Proc Natl Acad Sci USA 1980;77(12):7415–7419.
2. Gessain A, Barin F, Vernant JC, *et al.*: Antibodies to human T-lymphotropic virus type-I in patients with tropical spastic paraparesis. Lancet 1985;2:407–410.
3. Osame M, Usuku K, Izumo S, *et al.*: HTLV-I associated myelopathy, a new clinical entity. Lancet 1986;1(8488):1031–1032.
4. Uchiyama T, Yodoi J, Sagawa K, *et al.*: Adult T-cell leukemia: Clinical and hematologic features of 16 cases. Blood 1977;50(3):481–492.
5. Yoshida M, Seiki M, Yamaguchi K, *et al.*: Monoclonal integration of human T-cell leukemia provirus in all primary tumors of adult T-cell leukemia suggests causative role of human T-cell leukemia virus in the disease. Proc Natl Acad Sci USA 1984;81(8):2534–2537.
6. LaGrenade L, Hanchard B, Fletcher V, *et al.*: Infective dermatitis of Jamaican children: A marker for HTLV-I infection. Lancet 1990;336(8727):1345–1347.
7. Mariette X, Agbalika F, Zucker-Franklin D, *et al.*: Detection of the tax gene of HTLV-I in labial salivary glands from patients with Sjogren's syndrome and other diseases of the oral cavity. Clin Exp Rheumatol 2000;18(3):341–347.
8. Mochizuki M, Ono A, Ikeda E, *et al.*: HTLV-I uveitis. J Acquir Immune Defic Syndr Hum Retrovirol 1996;13(Suppl 1):S50–56.
9. Morgan OS, Rodgers-Johnson P, Mora C, *et al.*: HTLV-1 and polymyositis in Jamaica. Lancet 1989;2(8673):1184–1187.
10. Nishioka K, Maruyama I, Sato K, *et al.*: Chronic inflammatory arthropathy associated with HTLV-I. Lancet 1989;1(8635):441.
11. Kaplan TA: Low-lying disordered states when ground-state long-range order exists; large-amplitude spin waves. Phys Rev B Condens Matter 1990;41(10):6882–6888.
12. Murphy EL, Figueroa JP, Gibbs WN, *et al.*: Sexual transmission of human T-lymphotropic virus type I (HTLV-I). Ann Intern Med 1989;111(7):555–560.
13. Catalan-Soares B, Carneiro-Proietti AB, and Proietti FA: Heterogeneous geographic distribution of human T-cell lymphotropic viruses I and II (HTLV-I/II): Serological screening prevalence rates in blood donors from large urban areas in Brazil. Cad Saude Publica 2005;21(3):926–931.
14. Dourado I, Alcantara LC, Barreto ML, *et al.*: HTLV-I in the general population of Salvador, Brazil: A city with African ethnic and sociodemographic characteristics. J Acquir Immune Defic Syndr 2003;34(5):527–531.
15. Matsuura E, Yamano Y, and Jacobson S: Neuroimmunity of HTLV-I infection. J Neuroimmune Pharmacol 2010;5(3):310–325.
16. Araujo AQ and Silva MT: The HTLV-1 neurological complex. Lancet Neurol 2006;5(12):1068–1076.
17. Vernant JC, Maurs L, Gessain A, *et al.*: Endemic tropical spastic paraparesis associated with human T-lymphotropic virus type I: A clinical and seroepidemiological study of 25 cases. Ann Neurol 1987;21(2):123–130.
18. Lima MA, Bica RB, and Araujo AQ: Gender influence on the progression of HTLV-I associated myelopathy/tropical spastic paraparesis. J Neurol Neurosurg Psychiatry 2005;76(2):294–296.
19. Nakagawa M, Izumo S, Ijichi S, *et al.*: HTLV-I-associated myelopathy: Analysis of 213 patients based on clinical features and laboratory findings. J Neurovirol 1995;1(1):50–61.
20. Chang SC, Cheng JC, Kou YH, *et al.*: Roles of the AX(4)GKS and arginine-rich motifs of hepatitis C virus RNA helicase in ATP- and viral RNA-binding activity. J Virol 2000;74(20):9732–9737.
21. Taylor JM and Nicot C: HTLV-1 and apoptosis: Role in cellular transformation and recent advances in therapeutic approaches. Apoptosis 2008;13(6):733–747.
22. Richardson JH, Edwards AJ, Cruickshank JK, *et al.*: In vivo cellular tropism of human T-cell leukemia virus type 1. J Virol 1990;64(11):5682–5687.
23. Umehara F, Izumo S, Nakagawa M, *et al.*: Immunocytochemical analysis of the cellular infiltrate in the spinal cord lesions in HTLV-I-associated myelopathy. J Neuropathol Exp Neurol 1993;52(4):424–430.
24. Umehara F, Izumo S, Ronquillo AT, *et al.*: Cytokine expression in the spinal cord lesions in HTLV-I-associated myelopathy. J Neuropathol Exp Neurol 1994;53(1):72–77.
25. Goon PK, Igakura T, Hanon E, *et al.*: Human T cell lymphotropic virus type I (HTLV-I)-specific CD4+ T cells: Immunodominance hierarchy and preferential infection with HTLV-I. J Immunol 2004;172(3):1735–1743.
26. Nose H, Kubota R, Seth NP, *et al.*: Ex vivo analysis of human T lymphotropic virus type 1-specific CD4+ cells by use of a major histocompatibility complex class II tetramer composed of a neurological disease-susceptibility allele and its immunodominant peptide. J Infect Dis 2007;196(12):1761–1772.
27. De Castro-Costa CM, Araujo AQ, Barreto MM, *et al.*: Proposal for diagnostic criteria of tropical spastic paraparesis/HTLV-I-associated myelopathy (TSP/HAM). AIDS Res Hum Retroviruses 2006;22(10):931–935.
28. Pinto MT, Rodrigues ES, Malta TM, *et al.*: HTlV-1/2 Seroprevalence and coinfection rate in Brazilian first-time blood donors: An 11-year follow-up. Rev Inst Med Trop Sao Paulo 2012;54(3):123–129.
29. Vandesompele J, De Preter K, Pattyn F, *et al.*: Accurate normalization of real-time quantitative RT-PCR data by geometric averaging of multiple internal control genes. Genome Biol 2002;3(7):RESEARCH0034.
30. Pfaffl MW: A new mathematical model for relative quantification in real-time RT-PCR. Nucleic Acids Res 2001;29(9):e45.
31. Cao X, Cai SF, Fehniger TA, *et al.*: Granzyme B and perforin are important for regulatory T cell-mediated suppression of tumor clearance. Immunity 2007;27(4):635–646.
32. Ziegler SF: FOXP3: Of mice and men. Annu Rev Immunol 2006;24:209–226.
33. Goon PK, Hanon E, Igakura T, *et al.*: High frequencies of Th1-type CD4(+) T cells specific to HTLV-1 Env and Tax proteins in patients with HTLV-1-associated myelopathy/tropical spastic paraparesis. Blood 2002;99(9):3335–3341.
34. Hashimoto K, Higuchi I, Osame M, *et al.*: Quantitative in situ PCR assay of HTLV-1 infected cells in peripheral blood

lymphocytes of patients with ATL, HAM/TSP and asymptomatic carriers. J Neurol Sci 1998;159(1):67–72.
35. Kubota R, Kawanishi T, Matsubara H, *et al.:* Demonstration of human T lymphotropic virus type I (HTLV-I) tax-specific CD8+ lymphocytes directly in peripheral blood of HTLV-I-associated myelopathy/tropical spastic paraparesis patients by intracellular cytokine detection. J Immunol 1998;161(1): 482–488.
36. Nagai M, Usuku K, Matsumoto W, *et al.:* Analysis of HTLV-I proviral load in 202 HAM/TSP patients and 243 asymptomatic HTLV-I carriers: High proviral load strongly predisposes to HAM/TSP. J Neurovirol 1998; 4(6):586–593.
37. Vine AM, Heaps AG, Kaftantzi L, *et al.:* The role of CTLs in persistent viral infection: Cytolytic gene expression in CD8+ lymphocytes distinguishes between individuals with a high or low proviral load of human T cell lymphotropic virus type 1. J Immunol 2004;173(8):5121–5129.
38. Oliere S, Hernandez E, Lezin A, *et al.:* HTLV-1 evades type I interferon antiviral signaling by inducing the suppressor of cytokine signaling 1 (SOCS1). PLoS Pathog 2010;6(11): e1001177.
39. Fernandis AZ, Prasad A, Band H, *et al.:* Regulation of CXCR4-mediated chemotaxis and chemoinvasion of breast cancer cells. Oncogene 2004;23(1):157–167.
40. Hartmann TN, Burger JA, Glodek A, *et al.:* CXCR4 chemokine receptor and integrin signaling co-operate in mediating adhesion and chemoresistance in small cell lung cancer (SCLC) cells. Oncogene 2005;24(27):4462–4471.
41. Luker KE and Luker GD: Functions of CXCL12 and CXCR4 in breast cancer. Cancer Lett 2006;238(1):30–41.
42. Ganju RK, Brubaker SA, Meyer J, *et al.:* The alpha-chemokine, stromal cell-derived factor-1alpha, binds to the transmembrane G-protein-coupled CXCR-4 receptor and activates multiple signal transduction pathways. J Biol Chem 1998; 273(36):23169–23175.
43. Bustin SA: Quantification of mRNA using real-time reverse transcription PCR (RT-PCR): Trends and problems. J Mol Endocrinol 2002;29(1):23–39.
44. Chuaqui RF, Bonner RF, Best CJ, *et al.:* Post-analysis follow-up and validation of microarray experiments. Nat Genet 2002;32(Suppl):509–514.
45. Freeman WM, Walker SJ, and Vrana KE: Quantitative RT-PCR: Pitfalls and potential. Biotechniques 1999;26(1): 112–122, 124–125.
46. Wurmbach E, Yuen T, and Sealfon SC: Focused microarray analysis. Methods 2003;31(4):306–316.
47. Yang YH, Dudoit S, Luu P, *et al.:* Normalization for cDNA microarray data: A robust composite method addressing single and multiple slide systematic variation. Nucleic Acids Res 2002;30(4):e15.
48. Tan PK, Downey TJ, Spitznagel EL Jr, *et al.:* Evaluation of gene expression measurements from commercial microarray platforms. Nucleic Acids Res 2003;31(19):5676–5684.
49. Yauk CL, Berndt ML, Williams A, *et al.:* Comprehensive comparison of six microarray technologies. Nucleic Acids Res 2004;32(15):e124.
50. Zhu B, Ping G, Shinohara Y, *et al.:* Comparison of gene expression measurements from cDNA and 60-mer oligonucleotide microarrays. Genomics 2005;85(6):657–665.
51. Jazin EE, Soderstrom S, Ebendal T, *et al.:* Embryonic expression of the mRNA for the rat homologue of the fusin/CXCR-4 HIV-1 co-receptor. J Neuroimmunol 1997;79(2): 148–154.
52. Moepps B, Frodl R, Rodewald HR, *et al.:* Two murine homologues of the human chemokine receptor CXCR4 mediating stromal cell-derived factor 1alpha activation of Gi2 are differentially expressed in vivo. Eur J Immunol 1997; 27(8):2102–2112.
53. Ideker T, Thorsson V, Ranish JA, *et al.:* Integrated genomic and proteomic analyses of a systematically perturbed metabolic network. Science 2001;292(5518):929–934.
54. Greenbaum D, Colangelo C, Williams K, *et al.:* Comparing protein abundance and mRNA expression levels on a genomic scale. Genome Biol 2003;4(9):117.
55. Gygi SP, Rochon Y, Franza BR, *et al.:* Correlation between protein and mRNA abundance in yeast. Mol Cell Biol 1999;19(3):1720–1730.
56. Schwanhausser B, Busse D, Li N, *et al.:* Global quantification of mammalian gene expression control. Nature 2011; 473(7347):337–342.
57. Ghazalpour A, Bennett B, Petyuk VA, *et al.:* Comparative analysis of proteome and transcriptome variation in mouse. PLoS Genet 2011;7(6):e1001393.
58. Vogel C and Marcotte EM: Insights into the regulation of protein abundance from proteomic and transcriptomic analyses. Nat Rev Genet 2012;13(4):227–232.
59. Arai M, Ohashi T, Tsukahara T, *et al.:* Human T-cell leukemia virus type 1 Tax protein induces the expression of lymphocyte chemoattractant SDF-1/PBSF. Virology 1998; 241(2):298–303.
60. Kawaguchi A, Orba Y, Kimura T, *et al.:* Inhibition of the SDF-1alpha-CXCR4 axis by the CXCR4 antagonist AMD3100 suppresses the migration of cultured cells from ATL patients and murine lymphoblastoid cells from HTLV-I Tax transgenic mice. Blood 2009;114(14):2961–2968.
61. Pflanz S, Timans JC, Cheung J, *et al.:* IL-27, a heterodimeric cytokine composed of EBI3 and p28 protein, induces proliferation of naive CD4(+) T cells. Immunity 2002;16(6): 779–790.
62. Niedbala W, Cai B, Wei X, *et al.:* Interleukin 27 attenuates collagen-induced arthritis. Ann Rheum Dis 2008;67(10): 1474–1479.
63. Batten M, Li J, Yi S, *et al.:* Interleukin 27 limits autoimmune encephalomyelitis by suppressing the development of interleukin 17-producing T cells. Nat Immunol 2006;7(9): 929–936.
64. Hamano S, Himeno K, Miyazaki Y, *et al.:* WSX-1 is required for resistance to Trypanosoma cruzi infection by regulation of proinflammatory cytokine production. Immunity 2003; 19(5):657–667.
65. Stumhofer JS, Laurence A, Wilson EH, *et al.:* Interleukin 27 negatively regulates the development of interleukin 17-producing T helper cells during chronic inflammation of the central nervous system. Nat Immunol 2006;7(9):937–945.
66. Yoshimura T, Takeda A, Hamano S, *et al.:* Two-sided roles of IL-27: Induction of Th1 differentiation on naive CD4+ T cells versus suppression of proinflammatory cytokine production including IL-23-induced IL-17 on activated CD4+ T cells partially through STAT3-dependent mechanism. J Immunol 2006;177(8):5377–5385.
67. Fakruddin JM, Lempicki RA, Gorelick RJ, *et al.:* Noninfectious papilloma virus-like particles inhibit HIV-1 replication: Implications for immune control of HIV-1 infection by IL-27. Blood 2007;109(5):1841–1849.
68. Frank AC, Zhang X, Katsounas A, *et al.:* Interleukin-27, an anti-HIV-1 cytokine, inhibits replication of hepatitis C virus. J Interferon Cytokine Res 2010;30(6):427–431.

69. Greenwell-Wild T, Vazquez N, Jin W, *et al.:* Interleukin-27 inhibition of HIV-1 involves an intermediate induction of type I interferon. Blood 2009;114(9):1864–1874.
70. Imamichi T, Yang J, Huang DW, *et al.:* IL-27, a novel anti-HIV cytokine, activates multiple interferon-inducible genes in macrophages. AIDS 2008;22(1):39–45.
71. Larousserie F, Bardel E, Pflanz S, *et al.:* Analysis of interleukin-27 (EBI3/p28) expression in Epstein-Barr virus- and human T-cell leukemia virus type 1-associated lymphomas: Heterogeneous expression of EBI3 subunit by tumoral cells. Am J Pathol 2005;166(4):1217–1228.
72. Wang J, Wang G, Sun B, *et al.:* Interleukin-27 suppresses experimental autoimmune encephalomyelitis during bone marrow stromal cell treatment. J Autoimmun 2008;30(4):222–229.
73. Amadi-Obi A, Yu CR, Liu X, *et al.:* TH17 cells contribute to uveitis and scleritis and are expanded by IL-2 and inhibited by IL-27/STAT1. Nat Med 2007;13(6):711–718.
74. Miyazaki Y, Shimanoe Y, Wang S, *et al.:* Amelioration of delayed-type hypersensitivity responses by IL-27 administration. Biochem Biophys Res Commun 2008;373(3):397–402.
75. Grossman WJ, Verbsky JW, Barchet W, *et al.:* Human T regulatory cells can use the perforin pathway to cause autologous target cell death. Immunity 2004;21(4):589–601.
76. Zhao DM, Thornton AM, DiPaolo RJ, *et al.:* Activated CD4+CD25+ T cells selectively kill B lymphocytes. Blood 2006;107(10):3925–3932.
77. Hori S, Nomura T, and Sakaguchi S: Control of regulatory T cell development by the transcription factor Foxp3. Science 2003;299(5609):1057–1061.
78. Fontenot JD and Rudensky AY: A well adapted regulatory contrivance: Regulatory T cell development and the forkhead family transcription factor Foxp3. Nat Immunol 2005; 6(4):331–337.
79. Roncador G, Garcia JF, Maestre L, *et al.:* FOXP3, a selective marker for a subset of adult T-cell leukaemia/lymphoma. Leukemia 2005;19(12):2247–2253.
80. Oh U, Grant C, Griffith C, Fugo K, *et al.:* Reduced Foxp3 protein expression is associated with inflammatory disease during human T lymphotropic virus type 1 infection. J Infect Dis 2006;193(11):1557–1566.
81. Hayashi D, Kubota R, Takenouchi N, *et al.:* Reduced Foxp3 expression with increased cytomegalovirus-specific CTL in HTLV-I-associated myelopathy. J Neuroimmunol 2008; 200(1–2):115–124.
82. Toulza F, Heaps A, Tanaka Y, *et al.:* High frequency of CD4+FoxP3+ cells in HTLV-1 infection: Inverse correlation with HTLV-1-specific CTL response. Blood 2008;111(10): 5047–5053.
83. Best I, Lopez G, Verdonck K, *et al.:* IFN-gamma production in response to Tax 161-233, and frequency of CD4+ Foxp3+ and Lin HLA-DRhigh CD123+ cells, discriminate HAM/TSP patients from asymptomatic HTLV-1-carriers in a Peruvian population. Immunology 2009;128(1 Suppl): e777–786.
84. Malec M, van der Velden VH, Bjorklund E, *et al.:* Analysis of minimal residual disease in childhood acute lymphoblastic leukemia: Comparison between RQ-PCR analysis of Ig/TcR gene rearrangements and multicolor flow cytometric immunophenotyping. Leukemia 2004;18(10):1630–1636.
85. Corti B, Altimari A, Gabusi E, *et al.:* Potential of real-time PCR assessment of granzyme B and perforin up-regulation for rejection monitoring in intestinal transplant recipients. Transplant Proc 2005;37(10):4467–4471.
86. Sarwal MM, Jani A, Chang S, *et al.:* Granulysin expression is a marker for acute rejection and steroid resistance in human renal transplantation. Hum Immunol 2001;62(1):21–31.
87. Shin GT, Kim SJ, Lee TS, *et al.:* Gene expression of perforin by peripheral blood lymphocytes as a marker of acute rejection. Nephron Clin Pract 2005;100(3):c63–70.
88. Vlad G, Ho EK, Vasilescu ER, *et al.:* Anti-CD25 treatment and FOXP3-positive regulatory T cells in heart transplantation. Transpl Immunol 2007;18(1):13–21.
89. Shi R, Yang J, Jaramillo A, *et al.:* Correlation between interleukin-15 and granzyme B expression and acute lung allograft rejection. Transpl Immunol 2004;12(2):103–108.
90. Vukmanovic-Stejic M, Zhang Y, Cook JE, *et al.:* Human CD4+ CD25hi Foxp3+ regulatory T cells are derived by rapid turnover of memory populations in vivo. J Clin Invest 2006;116(9):2423–2433.
91. Satou Y, Utsunomiya A, Tanabe J, *et al.:* HTLV-1 modulates the frequency and phenotype of FoxP3+CD4+ T cells in virus-infected individuals. Retrovirology 2012;9:46.
92. Tachibana N, Okayama A, Ishizaki J, *et al.:* Suppression of tuberculin skin reaction in healthy HTLV-I carriers from Japan. Int J Cancer 1988;42(6):829–831.
93. Malta TM, Silva IT, Pinheiro DG, *et al.:* Altered expression of degranulation-related genes in CD8(+) T cells in human T lymphotropic virus Type I infection. AIDS Res Hum Retroviruses 2013;28:826–836.

Address correspondence to:
Simone Kashima
Regional Blood Center of Ribeirão Preto
Rua Tenente Catão Roxo, 2501
14051-140 Ribeirão Preto
São Paulo
Brazil

E-mail: skashima@hemocentro.fmrp.usp.br

OPEN

Citation: Blood Cancer Journal (2013) 3, e132; doi:10.1038/bcj.2013.30

www.nature.com/bcj

ORIGINAL ARTICLE

Oral administration of an HSP90 inhibitor, 17-DMAG, intervenes tumor-cell infiltration into multiple organs and improves survival period for ATL model mice

E Ikebe[1], A Kawaguchi[2,3,13], K Tezuka[4,13], S Taguchi[1,13], S Hirose[1], T Matsumoto[1], T Mitsui[1], K Senba[1], A Nishizono[1], M Hori[5], H Hasegawa[6], Y Yamada[6], T Ueno[4], Y Tanaka[7], H Sawa[3], W Hall[8], Y Minami[9], KT Jeang[10], M Ogata[11], K Morishita[12], H Hasegawa[2], J Fujisawa[4] and H Iha[1]

In the peripheral blood leukocytes (PBLs) from the carriers of the human T-lymphotropic virus type-1 (HTLV-1) or the patients with adult T-cell leukemia (ATL), nuclear factor kappaB (NF-κB)-mediated antiapoptotic signals are constitutively activated primarily by the HTLV-1-encoded oncoprotein Tax. Tax interacts with the I κB kinase regulatory subunit NEMO (NF-κB essential modulator) to activate NF-κB, and this interaction is maintained in part by a molecular chaperone, heat-shock protein 90 (HSP90), and its co-chaperone cell division cycle 37 (CDC37). The antibiotic geldanamycin (GA) inhibits HSP90's ATP binding for its proper interaction with client proteins. Administration of a novel water-soluble and less toxic GA derivative, 17-dimethylaminoethylamino-17-demethoxygeldanamycin hydrochloride (17-DMAG), to Tax-expressing ATL-transformed cell lines, C8166 and MT4, induced significant degradation of Tax. 17-DMAG also facilitated growth arrest and cellular apoptosis to C8166 and MT4 and other ATL cell lines, although this treatment has no apparent effects on normal PBLs. 17-DMAG also downregulated Tax-mediated intracellular signals including the activation of NF-κB, activator protein 1 or HTLV-1 long terminal repeat in Tax-transfected HEK293 cells. Oral administration of 17-DMAG to ATL model mice xenografted with lymphomatous transgenic Lck-Tax (Lck proximal promoter-driven Tax transgene) cells or HTLV-1-producing tumor cells dramatically attenuated aggressive infiltration into multiple organs, inhibited *de novo* viral production and improved survival period. These observations identified 17-DMAG as a promising candidate for the prevention of ATL progression.

Blood Cancer Journal (2013) **3,** e132; doi:10.1038/bcj.2013.30; published online 16 August 2013

Keywords: 17-DMAG; molecular chaperon; Tax; ATL; apoptosis; transgenic model

INTRODUCTION

Nuclear factor kappaB (NF-κB) is a transcription factor that regulates immune and antiapoptotic responses to multiple extracellular stresses.[1,2] Under normal conditions, most NF-κB molecules are sequestered in the cytoplasm by the inhibitor I κB. In response to cellular stress, I κB is rapidly phosphorylated by the NF-κB activator I κB kinase (IKK) and ubiquitylated for degradation by the proteasome. This frees NF-κB for translocation into the nucleus, where it directs the transcriptional activation of NF-κB-responsive genes.[3,4] IKK is comprised of three different subunits, IKKα, IKKβ and IKKγ/NEMO (NF-κB essential modulator). IKKγ is also known as NF-κB essential modulator (NEMO). NEMO trimerizes rapidly in response to extracellular stimuli, such as the pro-inflammatory cytokine tumor necrosis factor-α (TNF-α), and recruits the two catalytic subunits, IKKα/β, to form a highly phosphorylated active IKK holoenzyme.[5] Several genetic studies have shown that cytokine-triggered activation of what is termed the canonical NF-κB activation pathway is primarily dependent on NEMO and IKKβ,[6,7] whereas IKKα activity is required for the development of the skin, limbs and lymph nodes.[8,9] Upon stimulation, several accessory proteins are recruited to IKK, and the molecular size of this active IKK complex reaches more than 1 MDa.[10,11] The molecular chaperone heat-shock protein 90 (HSP90) and its co-chaperone cell division cycle 37 (CDC37) are components of this high molecular weight (HMW)-IKK complex, and they play crucial roles in maintaining the activity of the complex.[12] The antibiotic geldanamycin (GA) specifically binds to the ATPase domain of HSP90 and inhibits its function as a molecular chaperone, resulting in the efficient inhibition of TNF-α-mediated activation of NF-κB.[12,13]

The human T-lymphotropic virus type-1 (HTLV-1), which is the etiologic agent of adult T-cell leukemia (ATL), encodes the oncoprotein Tax.[14–16] Tax activates NF-κB by interacting

[1]Department of Infectious Diseases, Faculty of Medicine, Oita University, Yufu, Japan; [2]Department of Pathology, National Institute of Infectious Diseases, Musashimurayama, Japan; [3]Department of Molecular Pathobiology, 21st Century COE Program for Zoonosis Control, Hokkaido University Research Center for Zoonosis Control, Sapporo, Japan; [4]Department of Microbiology, Kansai Medical University, Moriguchi, Japan; [5]Department of Hematology, Ibaraki Prefectural Central Hospital, Kasama, Ibaraki, Japan; [6]Department of Laboratory Medicine, Nagasaki University Graduate School of Biomedical Sciences, Nagasaki, Japan; [7]Department of Immunology, Graduate School of Medicine, University of the Ryukyus, Nishihara, Japan; [8]Department of Medical Microbiology, Centre for Research in Infectious Diseases, Conway Institute of Biomolecular and Biomedical Research, University College Dublin, Dublin, Ireland; [9]Department of Biotechnology, Maebashi Institute of Technology, Maebashi, Japan; [10]Molecular Virology Section, Laboratory of Molecular Microbiology, National Institute of Allergy and Infectious Diseases, Bethesda, MD, USA; [11]Department of Hematology, Faculty of Medicine, Oita University, Yufu, Japan and [12]Division of Tumor and Cellular Biochemistry, Department of Medical Sciences, Faculty of Medicine, University of Miyazaki, Miyazaki, Japan. Correspondence: Dr H Iha, Department of Infectious Diseases, Faculty of Medicine, Oita University, 1-1 Idaigaoka, Hasama, Yufu, Oita 879-5593, Japan.
E-mail: hiha@oita-u.ac.jp
[13]These authors contributed equally to this work.
Received 25 June 2012; revised 24 June 2013; accepted 28 June 2013

physically with NEMO.[10,17] NF-κB activation mediated by this Tax–NEMO interaction is similar to that of the TNF-α-triggered 'canonical' pathway. Tax induces IKK phosphorylation, ubiquitylation and proteasome-dependent degradation of I κB, thereby inducing the translocation of NF-κB into the nucleus.[18,19] However, in contrast to the TNF-α-triggered canonical pathway, which is transient and mostly IKKβ dependent, Tax-mediated NF-κB activation is persistent and utilizes both the IKKα and IKKβ subunits.[20,21] From these observations, we speculated that oncogenic Tax-mediated activation of NF-κB is distinguishable from the canonical NF-κB activation pathway, and indeed, we have succeeded in inhibiting Tax-mediated NF-κB activation using selected sets of NEMO-mutant peptides.[11]

Those earlier studies led us to ask whether GA can inhibit Tax-mediated HMW-IKK formation and suppress NF-κB activation as has been demonstrated in the TNF-α-triggered canonical pathway. To address this, we treated ATL cell lines or HEK293 cells transfected with a Tax expression vector with GA or its less toxic derivative 17-dimethylaminoethylamino-17-demethoxygeldanamycin hydrochloride (17-DMAG).[22] We found that these HSP90 inhibitors downregulated Tax-mediated intracellular activity including the activation of NF-κB, activator protein 1 and HTLV-1 long terminal repeat (HTLV-1-LTR). These findings prompted us to investigate the molecular mechanisms by which HSP90 inhibitors disrupt Tax-mediated signaling in ATL cells. We found that the stability of Tax in ATL cells is heavily dependent on the HSP90/CDC37 chaperones and that Tax is rapidly degraded without these chaperones following the addition of HSP90 inhibitors. Apoptosis of ATL cells was also induced by GA and 17-DMAG. Finally, the oral administration of 17-DMAG to severe combined immunodeficient (SCID) mice transplanted with lymphomatous cells bearing Lck proximal promoter-driven Tax transgene (Lck-Tax) cells[23] markedly inhibited the aggressive infiltration of these Lck-Tax cells into multiple organs. The same procedure to the humanized NOG (huNOG) mice inoculated with HTLV-1-producing Jurkat cells also resulted in the suppression of *de novo* viral production and improved the survival period.

MATERIALS AND METHODS

Ethics statement

This study was carried out in strict accordance with the recommendations in the Guidelines for Proper Conduct of Animal Experiments, Science Council of Japan (http://www.scj.go.jp/en/animal/index.html). All procedures involving animals and their care were approved by the Animal Care Committee of Oita University, National Institute of Infectious Diseases and Kansai Medical University in accordance with the Regulations for Animal Experiments in Oita University (approval ID: 24-22).

Chemicals, cells and cell culture conditions

All chemicals used in this study including 17-DMAG[22] and cell lines or peripheral blood leukocytes (PBLs) were described in Supplementary Information.

Coimmunoprecipitation and immunoblot

One million cells of MT4 and C8166 treated with or without 17-DMAG and HEK293 cells transfected with each plasmid (maximum 1 μg) by FugeneHD (Roche Applied Science, Tokyo, Japan) for 40 h were lysed with coimmunoprecipitation (Co-IP) buffer. Each 200 μg of precleared (with 30 μl of protein G agarose, CalBiochem, Millipore Corporation, Billerica, MA, USA) lysates was incubated with 2 μg of rabbit polyclonal anti-HSP90 (Stressgen Bioreagents, Ann Arbor, MI, USA) or rabbit anti-FLAG antibody (Sigma-Aldrich, St Louis, MO, USA) for at least 3 h at 4° C. Antibody–protein G complexes were washed, resolved by sodium dodecyl sulfate-polyacrylamide gel electrophoresis and transferred onto a polyvinylidene difluoride membrane, and specific proteins were detected by monoclonal anti-Tax, -HSP90 (Stressgen), -Flag, -tubulin (Sigma) or polyclonal anti-IKKb (Cell Signaling Technology) antibodies, respectively.

Real-time quantitative reverse transcriptase-PCR by the LightCycler system

Total RNA from MT4 cells treated with or without 17-DMAG was isolated using ISOGEN (Wako Pure Chemical Industries, Ltd., Osaka, Japan), and contaminated DNA was removed. cDNA was constructed by the Thermoscript reverse transcriptase-PCR system (Invitrogen, Life Technologies Japan Co., Tokyo, Japan), and real-time quantitative PCRs for Tax and glucose-6-phosphate 1-dehydrogenase were performed on a Roche LC480 system (Roche) with indicated probe and primer sets.

Cell viability assay

Cell lines or PBLs from ATL patients or healthy donors were treated with 2.5 μM of 17-DMAG for 1–4 days. After every 24 h incubation, cell viabilities were counted with Cell Counting Kit (Dojindo Laboratories, Kumamoto, Japan).

Caspase-3/7 assay

Cells used in the 'cell viability assay' were also subjected for apoptosis activity with cappase-3/7 assay and GLOMAX 96 microplate luminometer (Promega KK, Tokyo, Japan).

Plasmids

The details of plasmid pSG5-Tax,[24] HSP90,[25] Cdc37,[26] CMV-Tax or LTR-Tax[11] and CoralHue-Tax or −CDC37 vectors (MBL Co. Ltd., Nagoya, Japan)[27] are described in Supplementary Information.

Luciferase assay

HEK293 cells were transfected with plasmid DNA mixture containing the reporter plasmids (NF-κB-Luc or HTLV-1-LTR-Luc[11] and RSV-β-galactosidase as a transfection indicator) and Tax expression vectors (pSG5-Tax, CMV-Tax or LTR-Tax) by FugeneHD. After 24 h incubation of the transfection, where indicated, 17-DMAG at concentrations listed in the figures was added, and cells were further incubated for 16 h. Cell lysates were subjected to the luciferase assay kit and GLOMAX 96.

Microscopic observation of cells

HEK293 cells were transfected with phmKGN-MC-Tax and phmKGC-MN-Cdc37 or its mutant −Cdc37(N200) or −Cdc37(N180) for 48 h and then treated with 1 μM of Hoechst 34442 (Sigma). Light and fluorescent (green fluorescent protein (GFP) or Hoechst 34442) microscopic observation and photography were performed by BZ-9000 Biorevo (Keyence Co. Ltd., Osaka, Japan).

Transfer of Lck-Tax transgenic cells to SCID mice and treatment with 17-DMAG

SCID mice were injected intraperitoneally with 2×10^6 Lck-Tax cells.[23] 17-DMAG was administered orally 5 days per week, with 5, 15 or 30 mg/kg for 2–3 weeks, and then mice were sacrificed for pathological examination.

HTLV-1 infection to huNOG and flow cytometric analysis of peripheral bloods

Suspension of irradiated 1×10^6 HTLV-1-producing JEX cells was inoculated intraperitoneally into huNOG mice[28] at the age between 24 and 28 weeks. Peripheral blood cells were routinely collected every 2 weeks after infection. Spleen, bone marrow and lymph node were collected, and PBLs were stained with florescent dye-conjugated antibodies against human cellular surface markers.

DNA isolation and quantification of proviral load

Genomic DNA was extracted from single cell suspension of tissue or peripheral blood followed by the conventional phenol extraction method. Proviral load was measured by quantitative PCR as previously described.[29]

Histopathological examination and immunohistochemistry

Tissues were directly fixed in the neutral buffered formalin (Sigma), embedded in paraffin, sectioned and stained with hematoxylin and eosin. Peripheral blood smears were prepared using Giemsa staining and examined by light microscopy.

For details, see Supplementary Information.

RESULTS

The NF-κB-activating Tax–HSP90–IKK ternary complex is disaggregated by HSP90 inhibitors that induce Tax degradation

The molecular chaperone HSP90 and its co-chaperone CDC37 are both recruited to IKK and play essential roles in TNF-α-triggered HMW-IKK formation and subsequent NF-κB activation. The addition of the HSP90-specific inhibitor GA completely suppresses NF-κB signaling.[12] As we previously demonstrated that the expression of Tax also resulted in the formation of a HMW-IKK complex for activating NF-κB,[11] we speculated that the inhibition of HSP90 function by GA would also affect Tax-mediated NF-κB signaling. First, using Tax-expressing MT4 cells, we confirmed the interaction of Tax with HSP90 in the same protein complex by Co-IP assays (Figure 1a). We then treated MT4 cells for 24 h with a newly developed, less toxic and water-soluble GA derivative, 17-DMAG,[22] to evaluate its effects on the formation of a Tax-induced ternary complex, Tax–HSP90–IKK. To our surprise, the amount of Tax in MT4 cells decreased progressively with increasing doses of 17-DMAG (Figure 1b, upper panel) despite no apparent changes in the amount of HSP90 in the same lysate (data not shown). Under these conditions, the interaction between HSP90 and IKKβ was clearly reduced with increasing doses of 17-DMAG (Figure 1b, middle panel), whereas the amount of HSP90 immunoprecipitated throughout this range of concentrations was unchanged (Figure 1b, lower panel).

We then examined the kinetics of Tax degradation in MT4 cells treated with 17-DMAG. Reductions in Tax levels were observed in cells treated for 12 h and continued over time until by 48 h, when the level of Tax became undetectable (Figure 1c). This 17-DMAG-induced Tax degradation stabilized I κBα, whereas another NF-κB inhibitor dexamethasone had no effects (Supplementary Figure 1). Tax degradation by 17-DMAG occurred prior to mRNA suppression as the marked decrease of Tax mRNA was not observed until 24 h after treatment (Figure 1d), whereas protein level of Tax was obviously decreased by 12 h (compare Figures 1c and d). Our previous study indicated that Tax degradation is partly induced by caspase,[30] and polyubiquitylation had little effects on its cellular stability.[31] We therefore re-evaluated which pathway is responsible for the 17-DMAG-induced Tax degradation (Figure 1e). Tax degradation was partly blocked by the caspase inhibitor zVAD-fmk[30] and by autophagy inhibitors 3-methyladenine (3-MA) and 5-aminoimidazole-4-carboxamide-1-b-D-ribofuranoside (AICAR)[32] but not by the proteasome inhibitor MG132. Similar findings were obtained from parallel studies using another ATL cell line, C8166 (data not shown), although more investigation is needed for fully understanding of Tax instability.

GA and its derivatives are known to suppress a variety of intracellular signaling pathways, including NF-κB activation by inhibiting IKK.[12,33] One of the most important functions of NF-κB is to protect cells from apoptotic stress. A portion of 2.5 μM of 17-DMAG is sufficient to induce Tax degradation (Figure 1c) and I κBα stabilization (Supplementary Figure 1), which implies the suppression of ATL cell growth; however, it is important to know whether this concentration is toxic to normal PBLs. We, therefore, confirmed the median inhibitory concentrations of 17-DMAG for several ATL or non-ATL cell lines along with normal PBLs.

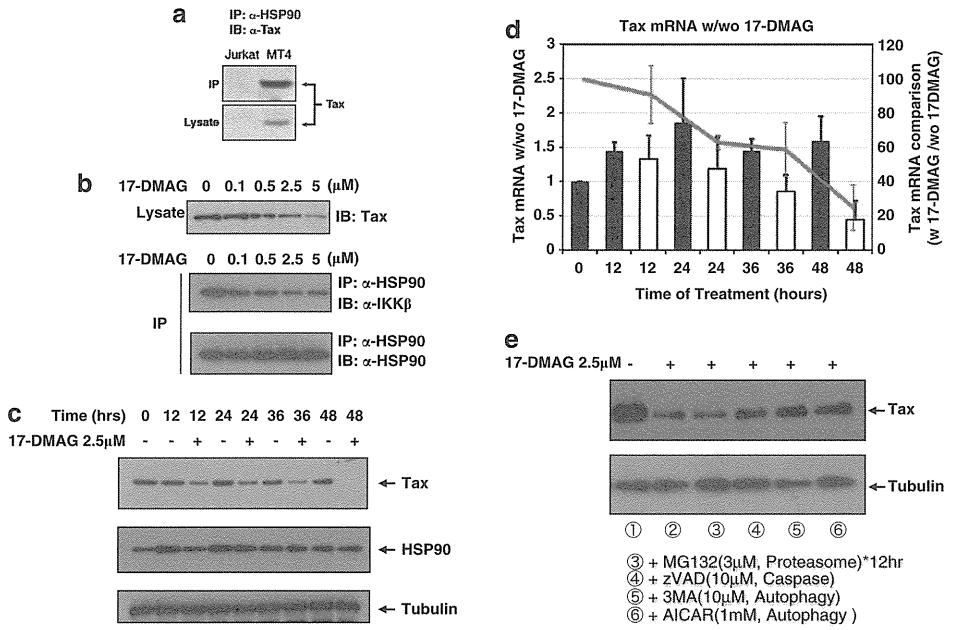

Figure 1. 17-DMAG inhibits HSP90–Tax–IKK ternary complex formation and induces Tax degradation in ATL cells. (**a**) Co-IP of Tax and HSP90. Four million Jurkat or MT4 cells were lysed with Co-IP buffer, and 50 μg total of cell lysates were subjected to IP with 2 μg of rabbit polyclonal anti-HSP90 antibody, followed by immunoblot (IB) with mouse monoclonal anti-Tax antibody (upper panel). The amount of expressed Tax in each cell line was verified by IB with anti-Tax against 10 μg of cell lysates (lower panel). (**b**) 17-DMAG's effects on Tax expression level and physical interaction between HSP90 and IKKβ in MT4 cells. Four million MT4 cells were treated with the indicated concentrations of 17-DMAG for 16 h. Co-IP and IB against immunoprecipitates or lysates were carried out as in panel **a**. (**c**) Ten micrograms of each cell lysate from MT4 cells treated with or without 2.5 μM of 17-DMAG for the indicated periods were subjected to sodium dodecyl sulfate-polyacrylamide gel electrophoresis, and Tax (upper panel), HSP90 (middle panel) or tubulin (lower panel) expression was detected using monoclonal anti-Tax, anti-HSP90 or anti-tubulin antibodies. (**d**) Expression levels of Tax in 17-DMAG-treated MT4 cells. mRNAs were prepared from the same aliquots of MT4 cells described in panel **c**. mRNAs from 17-DMAG-untreated fractions (black bars) and 17-DMAG-treated fractions (2.5 μM, white bars) with indicated time courses were analyzed with the universal probes (Roche) and primers through the LightCycler PCR method according to the manufacturer's direction. Comparison of Tax mRNAs with or without 17-DMAG was also indicated with a red line graph as a division of Tax mRNA with 17-DMAG/without 17-DMAG at each time point. (**e**) Four million MT4 cells were treated with 2.5 μM 17-DMAG for 24 h (lanes 2–6) and then additional 3 μM MG132 for 12 h (lane 3), 10 μM zVAD-fmk (lane 4) and 3-MA (lane 5) and 1 mM AICAR (lane 6) for 24 h. Lysates were prepared for IB of Tax and tubulin.

The median inhibitory concentrations to ATL cells vary from 0.06 to 2.33 μM, which is much lower than that of non-ATL Jurkat cells (9.32 μM), and three PBLs did not show any significant growth suppression with 10 μM of 17-DMAG (Supplementary Figure 2). We set the concentration of 17-DMAG at 2.5 μM and measured the effects on the viability of ATL cells (cell lines established from ATL patients' PBLs or cord blood cocultured with ATL patients' PBLs or primary PBLs of ATL patients) and other leukemic cells, as well as PBLs from HTLV-1-negative controls. Most of the ATL cell lines treated with 17-DMAG exhibited a rapid decrease in viability, whereas normal PBLs were unaffected by the drug (Figure 2a). 17-DMAG treatment also resulted in a marked increase in caspase-3/7 activity in most of the ATL cell lines while having no significant caspase perturbation in control PBLs (Figure 2b).

Downregulation of Tax occurs at the post-transcriptional stage

We then proceeded to examine the details of 17-DMAG-dependent inhibitory effects on the Tax–HSP90–IKK ternary complex by transfection of two different Tax expression vectors into HEK293 cells. One was driven by the simian virus 40 early promoter and

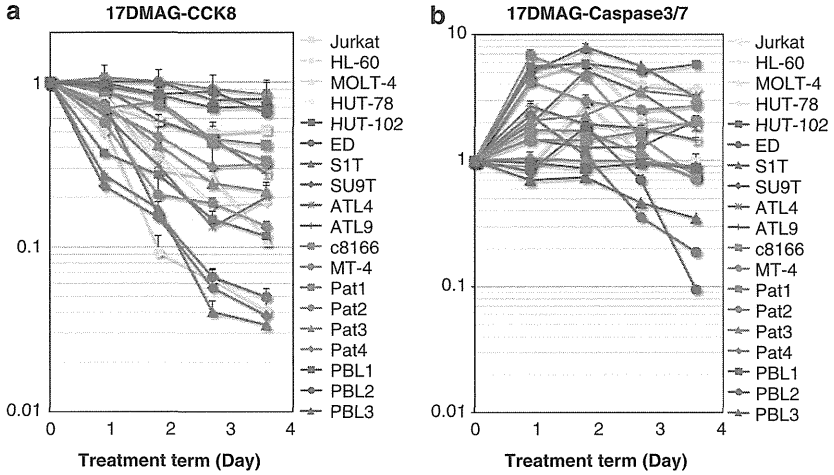

Figure 2. 17-DMAG induces growth arrest and apoptosis in ATL cells. Two million cells from each ATL cell line established from ATL patients' PBLs (HUT-102, ED, S1T, SU9T, ATL4 and ATL9; red lines), ATL cell lines established by coculture of cord blood and ATL patients' PBLs (C8166 and MT4; orange lines), PBLs from ATL patients (Pat1 to Pat4; purple lines), non-ATL leukemic cell lines (Jurkat, HL-60, MOLT-4 and HUT-78; yellow lines) or healthy donors (PBL1, PBL2 and PBL3; blue lines) were treated with 2.5 μM of 17-DMAG for 1–4 days. After each 24 h incubation, 10^4 (**a**) or 5×10^3 (**b**) cells were transferred to each well of a 96-well plate. (**a**) One-tenth volume of Cell Counting Kit 8 solution (Dojindo) was added to each fraction. Thirty minutes after incubation, the absorbance at 465 nm was measured using an E-max precision microplate reader (Molecular Devices Japan Co. Ltd., Tokyo, Japan). (**b**) The same volume of Apo-ONE homogeneous Caspase-3/7 assay solution was added to cells, and chemical luminescence was quantified with GloMax luminometer (Promega).

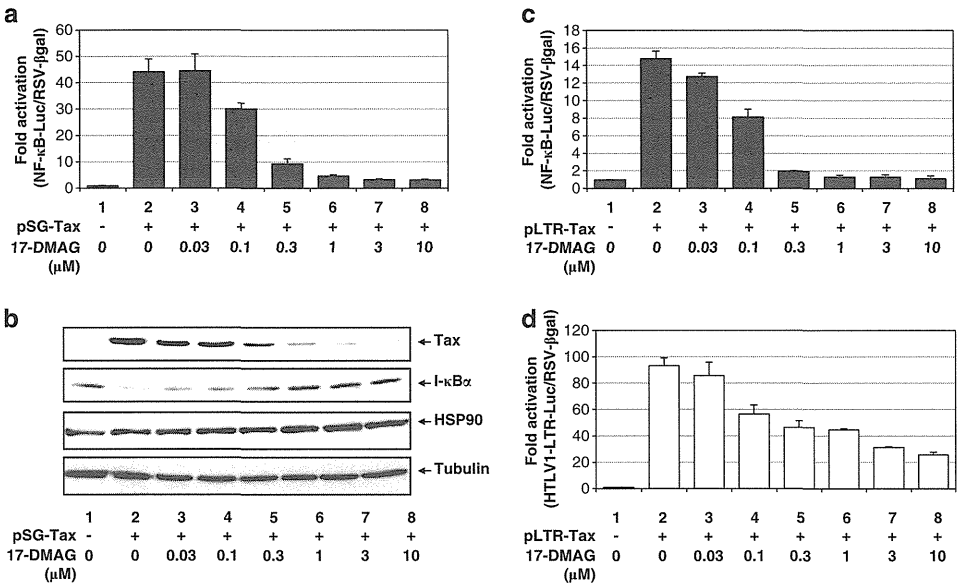

Figure 3. 17-DMAG downregulates all the Tax-mediated signaling in HEK293 cells. Fifty thousand HEK293 cells in each well on a 12-well plate were transfected with 0.5 μg of pSG-Tax (**a**, **c**) or pLTR-Tax along with 50 ng of NF-κB-luciferase (**a**, **c**) or HTLV-1-LTR-luciferase (**d**) and 50 ng of RSV-β-galactosidase control plasmid. A portion of 0.1–5 μM of 17-DMAG was added as indicated for 16 h. (**b**) The expression levels of Tax, HSP90 and tubulin in 10 μg of lysates from panel (**a**) were monitored by IB with monoclonal antibodies for each protein.

β-globin intron II (pSG5-Tax),[24] whereas the other was driven by the HTLV-1-LTR (LTR-Tax). These lines were transfected with either a NF-κB-responsive or a HTLV-1-LTR luciferase reporter (Figures 3a and b and Figures 3c and d, respectively) and RSV-β-galactosidase for readout normalization. 17-DMAG treatment was found to suppress Tax-mediated NF-κB (Figures 3a, b and c) or HTLV-1-LTR activation (Figure 3d) regardless of whether Tax was expressed from pSG5-Tax (Figures 3a and b) or LTR-Tax (Figures 3c and d). In these experiments, the ectopically expressed Tax from transfected plasmid was again downregulated by 17-DMAG (Figure 3b). The same results were also obtained from the cell lysates transfected with LTR-Tax or CMV-Tax (data not shown). In addition to these two enhancers, activator protein 1 activation by Tax[34] was also inhibited by 17-DMAG (data not shown). As the three discrete pathways

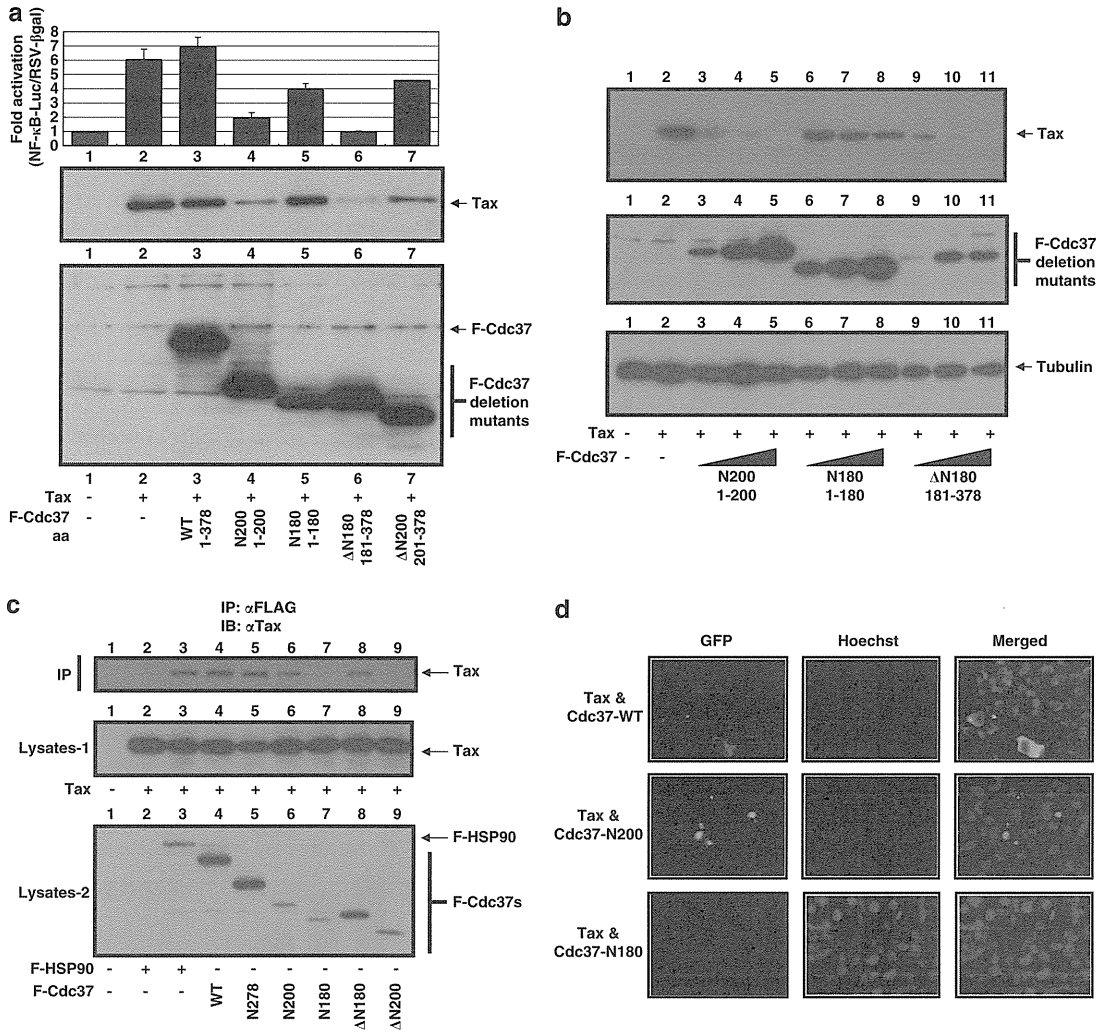

Figure 4. CBD of Cdc37 plays a crucial role for Tax stability in cells. (**a**) Co-transfection of LTR-Tax and pcDNA3-Flag-tagged Cdc37 (F-Cdc37) mutants. Lane 1: control pcDNA3 1 μg; lane 2: LTR-Tax 0.5 μg + pcDNA3 0.5 μg; lane 3: LTR-Tax 0.5 μg + F-Cdc37(1–378) wild type 0.5 μg; lane 4: LTR-Tax 0.5 μg + F-Cdc37(1–200) 0.5 μg; lane 5: LTR-Tax 0.5 μg + F-Cdc37(1–180) 0.5 μg; lane 6: LTR-Tax 0.5 μg + F-Cdc37(181–378) 0.5 μg; lane 7: LTR-Tax 0.5 μg + F-Cdc37(201–378) 0.5 μg. After 40 h transfection, HEK293 cells were lysed with 100 μl of lysis buffer, and the NF-κB-dependent luciferase activity was normalized with β-galactosidase value (upper panel). A portion of 10 μg of each lysate was resolved by sodium dodecyl sulfate-polyacrylamide gel electrophoresis, and the expression of Tax (middle panel) or Flag-tagged Cdc37s (lower panel) was detected by specific monoclonal antibodies. (**b**) Dose-dependent degradation of Tax by F-Cdc37 mutants. Lane 1: control pcDNA3 1 μg; lanes 2–11: 0.5 μg of LTR-Tax; lanes 3–5: plus 0.125, 0.25 and 0.5 μg of F-Cdc37(1–200); lanes 6–8: plus 0.125, 0.25 and 0.5 μg of F-Cdc37(1–180); lanes 9–11: plus 0.125, 0.25 and 0.5 μg of F-Cdc37(181–378). pcDNA3 was added to normalize the DNA amount. Tax (upper panel), Flag-tagged Cdc37s (middle panel) and tubulin (lower panel) were detected by specific monoclonal antibodies. (**c**) Cdc37's CBD (amino-acid residues 181–200(ref. 26)) is required for Tax interaction. A portion of 0.5 μg of control pcDNA3 (lane 1) or LTR-Tax (lanes 2–9) was transfected (lysate-1, middle panel) and 0.5 g of control pcDNA3 (lanes 1 and 2), F-HSP90 (lane 3), wild-type F-Cdc37(1–378, lane 4), F-Cdc37(1–278, lane 5), F-Cdc37(1–200, lane 6), F-Cdc37(1–180, lane 7), F-Cdc37(181–378, lane 8) and F-Cdc37(201–378, lane 9) were transfected separately (lysate-2, lower panel). The expression of each protein in cell lysates was detected by specific monoclonal antibodies (middle and bottom panels). A portion of 200 μg of each lane's cell lysates was mixed and subjected to Co-IP with 2 μg of rabbit anti-Flag antibodies, and each Co-IP complex was washed four times with Co-IP buffer, and following sodium dodecyl sulfate-polyacrylamide gel electrophoresis, Tax was detected by anti-Tax antibody (upper panel). (**d**) GFP two-hybrid binding assay between Cdc37 and Tax. HEK293 cells seeded on the six-well plates were transfected with phmKGN-MC-Tax and phmKGC-MN-Cdc37 or its mutant −Cdc37(N200) and −Cdc37(N180) by FugeneHD. After 48 h incubation, the transfected HEK293 cells were treated with Hoechst 34442 (Sigma) at the final concentration of 1 μM. Light and fluorescent (GFP and Hoechst 34442) microscopic observation and photography were performed by BZ-9000 Biorevo all-in-one fluorescence microscope (Keyence).

activated by Tax are inhibited by 17-DMAG treatment, the simplest interpretation suggests that all these effects arise from 17-DMAG-mediated destabilization of the Tax protein itself.

The client-binding domain of CDC37 plays crucial roles in Tax stabilization and Tax-mediated NF-κB activation

The molecular chaperone activity of HSP90 is usually exerted in cooperation with various co-chaperones. CDC37 was identified along with HSP90 as an essential component for a TNF-α-activated HMW-IKK complex.[12] As our current study shows the involvement of HSP90 in Tax-mediated HMW-IKK formation and NF-κB activation,[11,17] we generated Flag-tagged serial deletion mutants of HSP90 and CDC37 to examine their potential effects on Tax activity.

HSP90 has three distinct functional domains as described in Supplementary Figure 3.[35–37] We generated five deletion mutants, N, N + M, M, M + C and C, and transduced each with a Tax expression vector into HEK293 cells to determine any dominant-negative effects. Surprisingly, none of these mutants showed suppressive effects on Tax-mediated NF-κB activation or Tax stabilization (data not shown).

We then investigated the possible involvement of CDC37 in Tax stabilization and NF-κB signaling according to its functional domains (Supplementary Figure 3), namely, an HSP90-binding domain expanding through M164 to E221;[38] a kinase-binding domain at amino-acid residues 40–110;[39] a client-binding domain (CBD, amino-acid residues 181–200);[26] and a self-dimerization domain (amino-acid residues 240–260).[39] Although overexpression of full-length CDC37 slightly enhanced NF-κB activation (Figure 4a upper panel, lane 3), the mutants containing CBD, CDC37(1–200) and CDC37(181–378), strongly suppressed Tax-mediated NF-κB activation (Figure 4a upper panel, lanes 4 and 6) and induced extensive Tax degradation (Figure 4a middle panel, lanes 4 and 6). The mutants CDC37(1–180) and CDC37 (201–378) lacking CBD had little effects on either NF-κB activation or Tax stability (lanes 5 and 7). Tax degradation was reconfirmed by titration of these mutants (Figure 4b). Both CCD37(1–200) and CCD37 (181–378) progressively promoted Tax degradation (lanes 3–5 and 9–11, respectively), but CDC37(1–180) had little effects (lanes 6–8). Coexpression of certain sets of CDC37 mutants could promote Tax degradation through impaired physical interaction with Tax. We transfected HEK293 cells with Tax or Flag-CDC37 expression vectors separately to avoid spontaneous Tax degradation, and each cell lysate was mixed and applied for Co-IP experiments with anti-Flag antibodies (Figure 4c). Each protein expression was confirmed by immunoblotting for Tax (middle panel) or Flag (lower panel). Although the immunoprecipitates from wild-type HSP90 (upper panel, lane 3), CDC37 (lane 4) and Tax-degrading CDC37(1–200) and CDC37(181–378) (lanes 6 and 8) contained Tax in the complex, the immunoprecipitates from CDC37(1–180) and CDC37(201–378) lacking Tax-degrading properties did not (lanes 7 and 9).

Finally, we examined direct interaction between the two proteins using a GFP two-hybrid assay. Tax, tagged with the N-terminal portion of Kusabira-Green[27] fluorescent protein, and CDC37s (1–378, 1–200 and 1–180), tagged with the C-terminal portion, were co-transfected into HEK293 cells. Consistent with Co-IP results, co-transfectants of Tax and CDC37(1–378) or CDC37(1–200) emitted green fluorescence but Tax plus CDC37

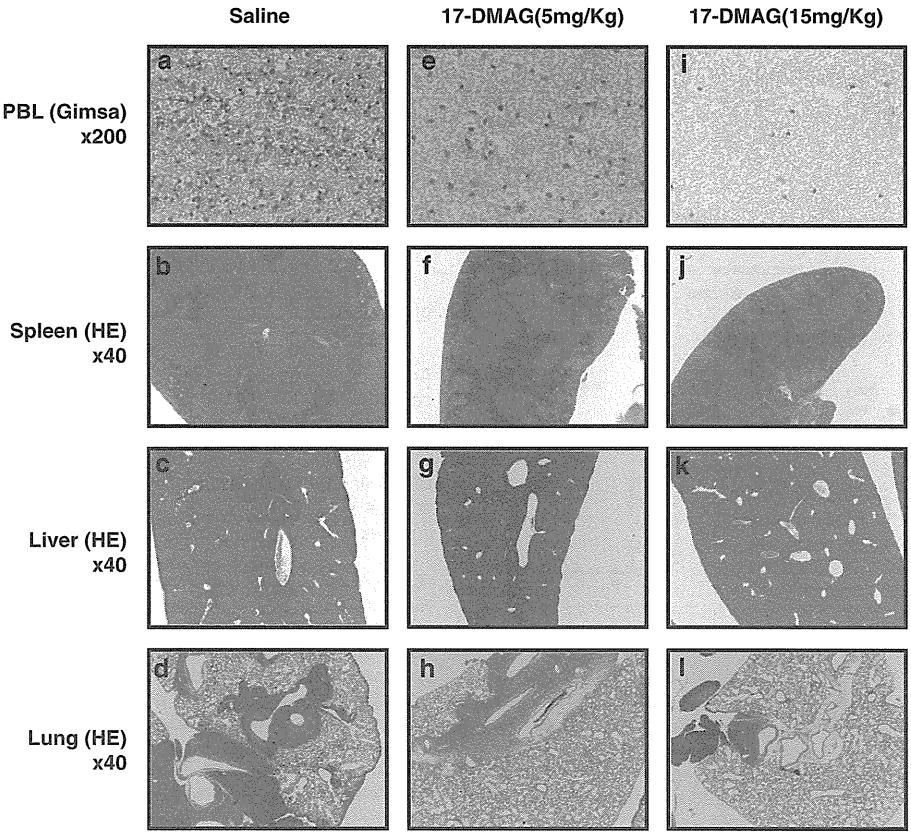

Figure 5. Oral administration of 17-DMAG blocks aggressive infiltration of Lck-Tax Tg cells into multiple organs of SCID mice. Two million Lck-Tax Tg cells were injected intraperitoneally into SCID mice. 17-DMAG was administered orally 5 days per week, with 5 mg/kg body weight (**e**–**h**) or 15 mg/kg body weight (**i**–**l**) or untreated (**a**–**d**). Mice were sacrificed after 21 days incubation, and organs were processed for Giemsa (**a**, **e**, **i**) or hematoxylin and eosin (HE, **b**–**d**, **f**–**h** and **j**–**l**) staining. Microscopic observations were performed and photographed with indicated magnifications. Tg, transgenic.

(1–180) did not. The Tax–CDC37(1–200) complex was translocated to the nucleus, whereas Tax–CDC37(1–378; wild type) stayed in the cytoplasm (Figure 4d). Collectively, these findings suggested the direct involvement of CDC37 for Tax stabilization.

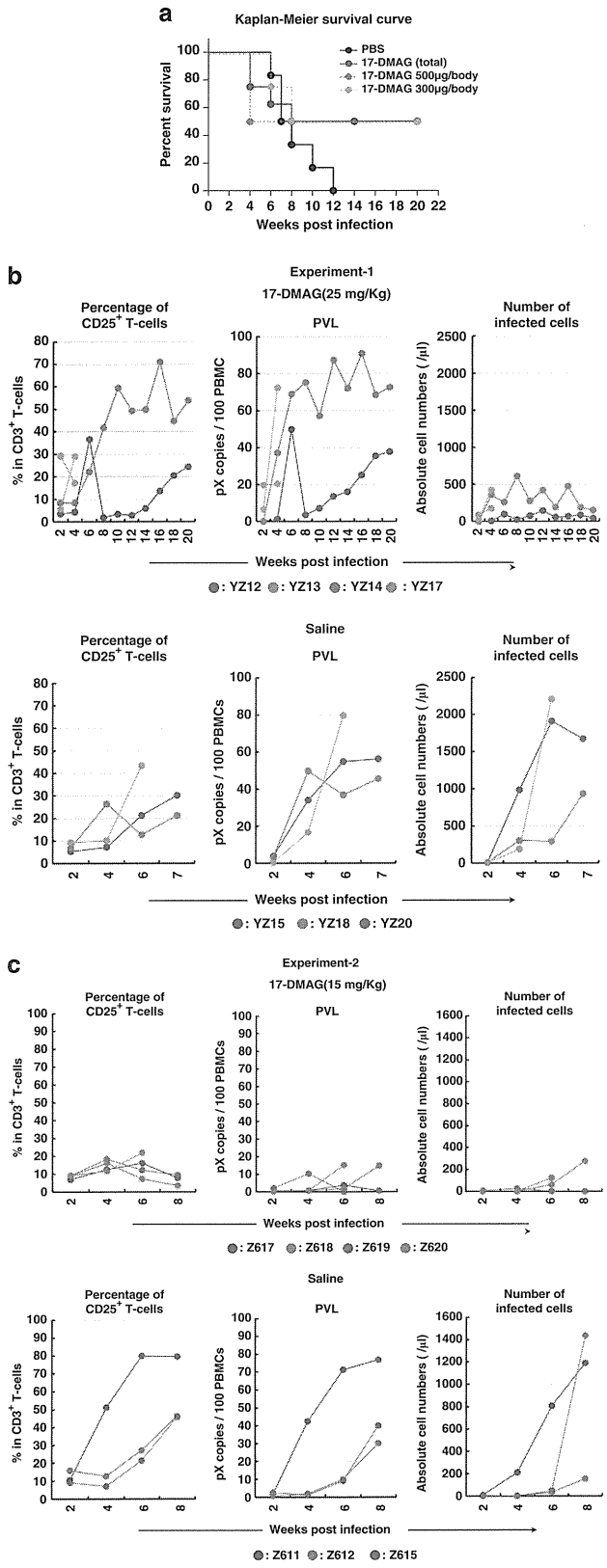

An oral administration of 17-DMAG to ATL model mice induced blockade of aggressive proliferation and multiple tissue invasions of transformed lymphocytes and improved survival rate

The demonstration that 17-DMAG has profound effects on Tax stability and the fact that it is water soluble suggested that this compound could be tested in a recently developed preclinical model of ATL.[23,28]

SCID mice were injected with 2×10^6 Lck-Tax cells intraperitoneally and treated for 5 consecutive days per week for 2 weeks with saline alone or with 17-DMAG in saline at 5 or 15 mg/kg. Mice were euthanized 21 days after cell inoculation. The blood smear indicated apparent reduction of Lck-Tax cells with increasing doses of 17-DMAG to saline controls (Figures 5a, e and i), although the quantitative cell counts were not obtained. The white pulp in greatly enlarged spleens (splenomegaly) of control mice was markedly expanded with red pulp compression (Figure 5b), and the livers and lungs of saline control mice were characterized by extensive perivascular infiltrations with Lck-Tax cells (Figures 5c and d). These pathologies were progressively reduced in mice treated with 17-DMAG (spleen, Figures 5f and j; liver, Figures 5g and k; and lung, Figures 5h and l).

We then determined the survival improvement through 17-DMAG oral administration with another preclinical ATL model (Figure 6). Each 7 (14 in total) huNOG mice[28] were injected with 1×10^6 HTLV-1-producing JEX cells (details are described in Supplementary Information), and 2 weeks after inoculation, each 4 of these mice (8 in total) were treated 20 times with 15 or 25 mg/kg of 17-DMAG for 4 weeks (as shown in Supplementary Figure 4), whereas the remaining 6 mice received saline only. The percentage of CD25-positive T cells, proviral load and the number of human leukocytes in peripheral blood were monitored. Four of eight 17-DMAG-treated mice died within 8 weeks post inoculation probably because of high drug dosage, but other four mice (50%) survived more than 20 weeks, whereas all the saline-treated controls died within 12 weeks post inoculation. The average survival period of controls and 17-DMAG-treated subjects were 8.33 and 14.75 weeks, respectively. However, the survival periods of 17-DMAG-treated subjects could be extended because four subjects were sacrificed at 24 weeks post inoculation for pathological examination (Supplementary Figure 4). The numbers of HTLV-1-infected human leukocytes in peripheral blood of 17-DMAG-treated subjects were also 5–10 times fewer than those of saline controls (Figures 6b and c).

Additive effects for growth arrest and apoptosis induction by concomitant 17-DMAG/Nutlin-3a treatment against ATL cells

The standard chemotherapy against ATL, named as leukemia study group 15 (LSG15), is currently employing the combination of four different anticancer drugs that frequently brings serious side effects to patients.[40] We previously demonstrated that a novel MDM-2-antagonizing/p53-stabilizing drug, Nutlin-3a, induces

Figure 6. Improved survival and suppression of the growth of HTLV-1-infected T cells by 17-DMAG oral treatment. (**a**) Kaplan–Meier survival curve of HTLV-1-infected huNOG mice. All mice have reconstituted human immune system by the transplantation of hematopoietic stem cells (huNOG) and have received 1 million JEX cells, which produce HTVL-1 infectious virus (see the details in Supplementary Figure 4). JEX/huNOG mice received 17-DMAG by oral administration for 4 weeks (2–6 weeks post inoculation, five times/week) at the dosage of 25 mg/kg (orange line) and 15 mg/kg (pink line). Control mice received the same volume of PBS. (**b**) The percentage of CD25-positive T cells, PVL and the number of HTLV-1-infected cells in peripheral blood of infected mice are shown. Upper panel represents the results from 17-DMAG-treated (25 mg/kg) mice; lower panel represents those of control mice. (**c**) Same experiments with 17-DMAG (15 mg/kg, upper panel) and PBS control (lower panel). PBS, phosphate buffered saline; PVL, proviral load.

the senescent death to ATL cells.[41] We then examined the additive anti-ATL effects of 17-DMAG and Nutlin-3a. Suboptimal dose of 17-DMAG (0.1 μM) or Nutlin-3a (1 μM) alone did not induce sufficient apoptotic or growth-arrest activities to ATL cell lines. However, the combined use of both induced significant growth suppressive and apoptotic properties (Figure 7), suggesting the possible combinational use of these drugs for further clinical studies.

DISCUSSION

HTLV-1 is the etiologic agent of ATL. Current studies indicate that worldwide there are more than 20 million HTLV-1 carriers and that 5% of these carriers will develop ATL.[42] The current standard for treatment of acute- or lymphoma-type ATL in Japan is CHOP or its modified regimen LSG15; however, the responses to this treatment regimen are limited to 31.1% of patients with 2-year survivals.[40] As malignant cells from relapsed patients are also resistant to other chemotherapeutic interventions, novel strategies for treatment of ATL are urgently required.

In this study, we demonstrated the significant inhibitory effects of 17-DMAG on Tax-mediated NF-κB signaling *in vitro* and *ex vivo*. The most striking observations obtained *in vitro* were (a) 17-DMAG-induced Tax degradation that resulted from inhibiting the formation of the Tax–IKK–HSP90/CDC37 ternary complex (Figures 1a–d); (b) induction of growth suppression and apoptosis of ATL cells while having little or no effect on normal PBLs (Figures 2a and b). We also found that the stability of Tax was heavily dependent on the CBD of CDC37 (Figures 4a and b). GA-dependent NF-κB downregulation in ATL cells was reported, and inhibition of autophagic activity seemed to affect the conversion of p100 (NF-κB2 precursor) to active p52.[32] We observed this time 17-DMAG-dependent Tax degradation and its blockade by AICAR and 3-MA (autophagy inhibitors) but not by the proteasome inhibitor MG-132 (Figure 1d), suggesting the direct involvement of the autophagosome on Tax metabolism in cells. This issue should further be investigated with ubiquitylation-deficient mutants Tax[24,31] or the autophagy-deficient cells.[43,44]

The CBD of CDC37 has been reported to bind preferentially to a specific glycine-rich motif — GXGXXG.[45] Indeed, Tax has a similar motif in its N terminus. CBD played crucial roles in stabilizing Tax and Tax–CDC37 complex formation (Figures 4c and d). CBD-containing mutants of CDC37 seemed to enhance the machinery responsible for Tax degradation as we did not detect any decrease in Tax levels in response to an siRNA knockdown of CDC37 (Supplementary Figure 5). Interestingly, the Tax-destabilizing CDC37(N200) translocated Tax to the nucleus, whereas wild-type CDC37 stayed with Tax in the cytoplasm (Figure 4d), and it implies that this translocation could be related to the Tax destabilization. For the future, it would be worth trying to identify a chemical compound that mimics the structure of CBD and could function as an inducer of Tax degradation. HSP90 and its co-chaperone's involvement in multiple signaling cascades, especially, in cancer cells, has been reported.[46,47] Indeed, 17-DMAG also suppressed NF-κB signaling mediated by other activators NIK, MEKK1, AKT, TAB2 and IKKα/β (data not shown). We also found that 17-DMAG treatment induced Tax degradation; potentially 17-DMAG treatment may also have led to the destabilization of other NF-κB signaling activators.

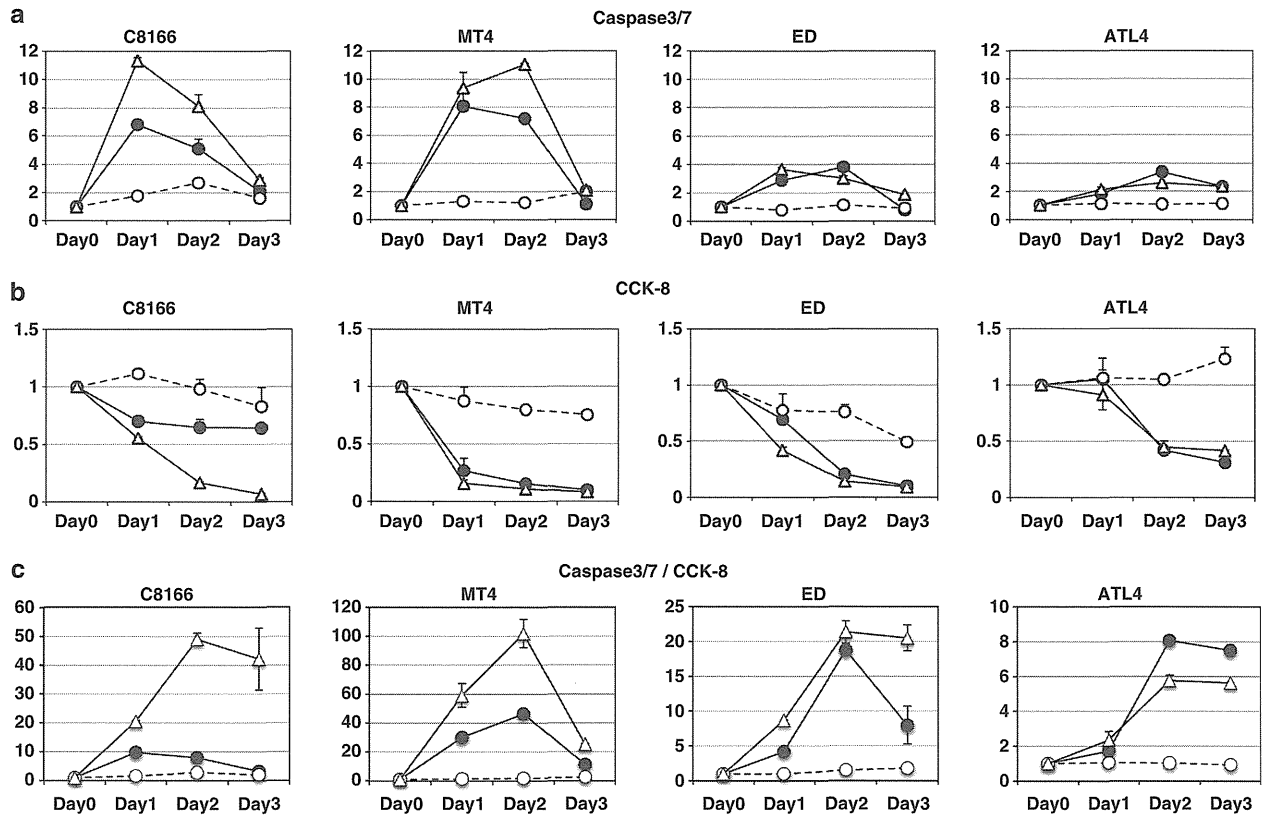

Figure 7. Additive anti-ATL cell effects by the combined dosage of 17-DMAG and Nutlin-3a. (**a**) ATL cell lines C8166, MT4, ED and ATL4 were treated with either suboptimal single dose of 17-DMAG (0.1 μM, black circles) and Nutlin-3a (1 μM, white circles)[41] or both (white triangles) for 3 days and harvested for caspase-3/7 assays (**a**) or CCK-8 assays (**b**) as described in Figure 2. Each untreated cell's value was set as 1. (**c**) Each caspase-3/7 (apoptotic) value was divided by CCK-8 (growth arrest) value to manifest the additive effects (see the Discussion section). CCK-8, Cell Counting Kit 8.

We have determined the therapeutic effects of 17-DMAG on two different ATL model systems through its oral administration. First, we tested 17-DMAG induced prevention of Lck-Tax infiltration in SCID mice, and 5 and 15 mg/kg of oral administration of 17-DMAG for 2 weeks reduced 74% and 83% of Lck-Tax cells, respectively; splenomegaly or massive infiltration of Lck-Tax cells into livers and lungs was also significantly reduced (Figure 5). In all experiments, 17-DMAG mice did not show any body weight losses or inactiveness compared with saline controls.

We then switched to another ATL model experiment JEX/huNOG, which has humanized immune environment in NOG mice and has inoculated HTLV-1-producing Jurkat cells. With oral administration of both 15 and 25 mg/kg 17-DMAG to JEX/huNOG, four of eight mice survived more than 20 weeks, whereas saline controls died within 12 weeks (Figure 6a). 17-DMAG treatment also reduced the number of HTLV-1-infected cells in peripheral blood, suggesting that 17-DMAG treatment could intervene the clonal T-cell development to ATL (Figure 6b). Although this preliminary experiment did not provide statistically significant survival rates, efficacy of this treatment is indeed highly expected. It is necessary to find the optimized conditions suppressing the ATL cell proliferation without any serious side effects.

Tax has pleiotropic effects on intra-cellular or inter-cellular signalings including mitotic checkpoint disruption,[48] aberrant cell-cycle progression[49,50] and altered chemotaxis.[51] The present ATL treatment protocols target the cytoskeletons or DNA replications with multiple doses of anticancer drugs (called as LSG15), and significant side effects by this treatment have been frequently recognized.[40] We have recently demonstrated the potential uses of molecularly targeted inhibitors of ATL cell proliferation, such as a MDM-2 ubiquitin ligase inhibitor Nutlin-3a[41] or CXCR4 antagonist AMD3100.[51] Nutlin-3a induces growth arrest and senescent-cell death of ATL cells at the 10 μM concentration, but normal PBLs are also significantly affected.[41] The combined use of 17-DMAG (0.1 μM) and Nutlin-3a (1 μM), suboptimal concentration for single use, significantly enhanced both apoptotic and growth suppressive effects (Figures 7a and b). This concurrent effects can be manifested with the division of caspase-3/7 values by Cell Counting Kit 8 values (Figure 7c). Besides Nutlin-3a, we also tested the efficacy of 17-DMAG plus LSG15 (without predonisolone; Supplementary Figure 6). Unlike the results of 17-DMAG/Nutlin-3a, 17-DMAG/LSG15 did not show any clear additive effects probably because LSG15 affects cell-cycle progression with a wide range of spectrum, but the effects of Nutlin-3a are specifically restricted to p53 stabilization.

It remains to be seen whether 17-DMAG is effective for ATL patients' treatment; elsewhere Hertlein *et al.*[52] have reported 17-DMAG's clinical application against chronic lymphocytic leukemia. Perhaps in future studies, 17-DMAG and other new drugs with novel anti-ATL activities such as Nutlin-3a, AMD3100 or a monoclonal anti-CCR4 antibody (KW-0761)[53] will provide more effective and less toxic ATL therapy.

CONFLICT OF INTEREST

The authors declare no conflict of interest.

ACKNOWLEDGEMENTS

We are indebted to Dr Herbert C Morse III for his helpful discussion and comments. We thank Mr T Kawashima and Ms Y Itoh for technical assistance and Drs K Terasawa, C Pique and K Nagata for providing plasmid DNAs. EI was a research fellow of the Okinawa Science and Technology Promotion Center. This study was supported in part by grants from the Ministry of Education, Culture, Sports, Science and Technology; the Ministry of Health, Labor and Welfare; the Ministry of Economy, Trade and Industry; Japan Science and Technology Agency; Okinawa Science and Technology Promotion Center; and Miyazaki Prefectural Industrial Support Foundation.

AUTHOR CONTRIBUTIONS

HI, J-IF and HdH designed the research; HdH, HS, WWH, KT, TU and J-IF developed the ATL animal model; EI, AK, KT, ST, SH, TMa, TU, TMi, KS, J-IF, HdH and HI performed the research; AN, MH, HrH, YY, YT, HS, WH, YM, KTJ, MO and KM contributed new reagents/materials; AK, KT, J-IF and HdH contributed pathologic analysis; and EI, KT, J-IF, HdH and HI wrote the paper.

REFERENCES

1 Li Q, Verma IM. NF-kappaB regulation in the immune system. *Nat Rev Immunol* 2002; **2**: 725–734.
2 Janssens S, Tschopp J. Signals from within: the DNA-damage-induced NF-kappaB response. *Cell Death Differ* 2006; **13**: 773–784.
3 Karin M. NF-kappaB as a critical link between inflammation and cancer. *Cold Spring Harb Perspect Biol* 2009; **1**: a000141.
4 Hayden MS, Ghosh S. Shared principles in NF-kappaB signaling. *Cell* 2008; **132**: 344–362.
5 Li XH, Fang X, Gaynor RB. Role of IKK-gamma/NEMO in assembly of the I-kappaB kinase complex. *J Biol Chem* 2001; **276**: 4494–4500.
6 Li Q, Van Antwerp D, Mercurio F, Lee KF, Verma IM. Severe liver degeneration in mice lacking the I-kappaB kinase 2 gene. *Science* 1999; **284**: 321–325.
7 Schmidt-Supprian M, Bloch W, Courtois G, Addicks K, Israel A, Rajewsky K *et al.* NEMO/IKK-gamma-deficient mice model incontinentia pigmenti. *Mol Cell* 2000; **5**: 981–992.
8 Li Q, Lu Q, Hwang JY, Buscher D, Lee KF, Izpisua-Belmonte JC *et al.* IKK1-deficient mice exhibit abnormal development of skin and skeleton. *Genes Dev* 1999; **13**: 1322–1328.
9 Takeda K, Takeuchi O, Tsujimura T, Itami S, Adachi O, Kawai T *et al.* Limb and skin abnormalities in mice lacking IKK-alpha. *Science* 1999; **284**: 313–316.
10 Yamaoka S, Courtois G, Bessia C, Whiteside ST, Weil R, Agou F *et al.* Complementation cloning of NEMO, a component of the I-kappaB kinase complex essential for NF-kappaB activation. *Cell* 1998; **93**: 1231–1240.
11 Iha H, Kibler KV, Yedavalli VR, Peloponese JM, Haller K, Miyazato A *et al.* Segregation of NF-kappaB activation through NEMO/IKK-gamma by Tax and TNF-alpha: implications for stimulus-specific interruption of oncogenic signaling. *Oncogene* 2003; **22**: 8912–8923.
12 Chen G, Cao P, Goeddel DV. TNF-induced recruitment and activation of the IKK complex require Cdc37 and Hsp90. *Mol Cell* 2002; **9**: 401–410.
13 Bouwmeester T, Bauch A, Ruffner H, Angrand PO, Bergamini G, Croughton K *et al.* A physical and functional map of the human TNF-alpha/NF-kappa B signal transduction pathway. *Nat Cell Biol* 2004; **6**: 97–105.
14 Yoshida M. Multiple viral strategies of HTLV-1 for dysregulation of cell growth control. *Annu Rev Immunol* 2001; **19**: 475–496.
15 Hall WW, Fujii M. Deregulation of cell-signaling pathways in HTLV-1 infection. *Oncogene* 2005; **24**: 5965–5975.
16 Matsuoka M, Jeang KT. Human T-cell leukaemia virus type 1 (HTLV-1) infectivity and cellular transformation. *Nat Rev Cancer* 2007; **7**: 270–280.
17 Jin DY, Giordano V, Kibler KV, Nakano H, Jeang KT. Role of adapter function in oncoprotein-mediated activation of NF-kappaB. Human T-cell leukemia virus type I Tax interacts directly with I-kappaB kinase gamma. *J Biol Chem* 1999; **274**: 17402–17405.
18 Carter RS, Pennington KN, Ungurait BJ, Ballard DW. *In vivo* identification of inducible phosphoacceptors in the IKK-gamma/NEMO subunit of human I-kappaB kinase. *J Biol Chem* 2003; **278**: 19642–19648.
19 Lamsoul I, Lodewick J, Lebrun S, Brasseur R, Burny A, Gaynor RB *et al.* Exclusive ubiquitination and sumoylation on overlapping lysine residues mediate NF-kappaB activation by the human T-cell leukemia virus Tax oncoprotein. *Mol Cell Biol* 2005; **25**: 10391–10406.
20 Chu ZL, DiDonato JA, Hawiger J, Ballard DW. The Tax oncoprotein of human T-cell leukemia virus type 1 associates with and persistently activates I-kappaB kinases containing IKK-alpha and IKK-beta. *J Biol Chem* 1998; **273**: 15891–15894.
21 Geleziunas R, Ferrell S, Lin X, Mu Y, Cunningham Jr ET, Grant M *et al.* Human T-cell leukemia virus type 1 Tax induction of NF-kappaB involves activation of the I-kappaB kinase alpha (IKK-alpha) and IKK-beta cellular kinases. *Mol Cell Biol* 1998; **18**: 5157–5165.
22 Egorin MJ, Lagattuta TF, Hamburger DR, Covey JM, White KD, Musser SM *et al.* Pharmacokinetics, tissue distribution, and metabolism of 17-(dimethylaminoethylamino)-17-demethoxygeldanamycin (NSC 707545) in CD2F1 mice and Fischer 344 rats. *Cancer Chemother Pharmacol* 2002; **49**: 7–19.
23 Hasegawa H, Sawa H, Lewis MJ, Orba Y, Sheehy N, Yamamoto Y *et al.* Thymus-derived leukemia–lymphoma in mice transgenic for the Tax gene of human T-lymphotropic virus type I. *Nat Med* 2006; **12**: 466–472.

24 Chiari E, Lamsoul I, Lodewick J, Chopin C, Bex F, Pique C. Stable ubiquitination of human T-cell leukemia virus type 1 tax is required for proteasome binding. *J Virol* 2004; **78**: 11823–11832.
25 Momose F, Naito T, Yano K, Sugimoto S, Morikawa Y, Nagata K. Identification of Hsp90 as a stimulatory host factor involved in influenza virus RNA synthesis. *J Biol Chem* 2002; **277**: 45306–45314.
26 Terasawa K, Minami Y. A client-binding site of Cdc37. *FEBS J* 2005; **272**: 4684–4690.
27 Ueyama T, Kusakabe T, Karasawa S, Kawasaki T, Shimizu A, Son J *et al.* Sequential binding of cytosolic Phox complex to phagosomes through regulated adaptor proteins: evaluation using the novel monomeric Kusabira-Green system and live imaging of phagocytosis. *J Immunol* 2008; **181**: 629–640.
28 Nie C, Sato K, Misawa N, Kitayama H, Fujino H, Hiramatsu H *et al.* Selective infection of CD4+ effector memory T lymphocytes leads to preferential depletion of memory T lymphocytes in R5 HIV-1-infected humanized NOD/SCID/IL-2Rgammanull mice. *Virology* 2009; **394**: 64–72.
29 Ueno S, Umeki K, Takajo I, Nagatomo Y, Kusumoto N, Umekita K *et al.* Proviral loads of human T-lymphotropic virus type 1 in asymptomatic carriers with different infection routes. *Int J Cancer* 2012; **130**: 2318–2326.
30 De Valck D, Jin DY, Heyninck K, Van de Craen M, Contreras R, Fiers W *et al.* The zinc finger protein A20 interacts with a novel anti-apoptotic protein which is cleaved by specific caspases. *Oncogene* 1999; **18**: 4182–4190.
31 Peloponese JM, Iha H, Yedavalli VR, Miyazato A, Li Y, Haller K *et al.* Ubiquitination of human T-cell leukemia virus type 1 tax modulates its activity. *J Virol* 2005; **78**: 11686–11695.
32 Yan P, Qing G, Qu Z, Wu CC, Rabson A, Xiao G. Targeting autophagic regulation of NFkappaB in HTLV-I transformed cells by geldanamycin: implications for therapeutic interventions. *Autophagy* 2007; **3**: 600–603.
33 Mitsiades CS, Mitsiades NS, McMullan CJ, Poulaki V, Kung AL, Davies FE *et al.* Antimyeloma activity of heat shock protein-90 inhibition. *Blood* 2006; **107**: 1092–1100.
34 Jeang KT, Chiu R, Santos E, Kim SJ. Induction of the HTLV-I LTR by Jun occurs through the Tax-responsive 21-bp elements. *Virology* 1991; **181**: 218–227.
35 Prodromou C, Roe SM, O'Brien R, Ladbury JE, Piper PW, Pearl LH. Identification and structural characterization of the ATP/ADP-binding site in the Hsp90 molecular chaperone. *Cell* 1997; **90**: 65–75.
36 Meyer P, Prodromou C, Hu B, Vaughan C, Roe SM, Panaretou B *et al.* Structural and functional analysis of the middle segment of hsp90: implications for ATP hydrolysis and client protein and cochaperone interactions. *Mol Cell* 2003; **11**: 647–658.
37 Minami Y, Kimura Y, Kawasaki H, Suzuki K, Yahara I. The carboxy-terminal region of mammalian HSP90 is required for its dimerization and function *in vivo*. *Mol Cell Biol* 1994; **14**: 1459–1464.
38 Roe SM, Ali MM, Meyer P, Vaughan CK, Panaretou B, Piper PW *et al.* The mechanism of Hsp90 regulation by the protein kinase-specific cochaperone p50(cdc37). *Cell* 2004; **116**: 87–98.
39 Silverstein AM, Grammatikakis N, Cochran BH, Chinkers M, Pratt WB. p50(cdc37) binds directly to the catalytic domain of Raf as well as to a site on hsp90 that is topologically adjacent to the tetratricopeptide repeat binding site. *J Biol Chem* 1998; **273**: 20090–20095.
40 Uozumi K. Treatment of adult T-cell leukemia. *J Clin Exp Hematop* 2010; **50**: 9–25.
41 Hasegawa H, Yamada Y, Iha H, Tsukasaki K, Nagai K, Atogami S *et al.* Activation of p53 by Nutlin-3a, an antagonist of MDM2, induces apoptosis and cellular senescence in adult T-cell leukemia cells. *Leukemia* 2009; **23**: 2090–2101.
42 Proietti FA, Carneiro-Proietti AB, Catalan-Soares BC, Murphy EL. Global epidemiology of HTLV-I infection and associated diseases. *Oncogene* 2005; **24**: 6058–6068.
43 Mizushima N, Yoshimori T, Ohsumi Y. The role of Atg proteins in autophagosome formation. *Annu Rev Cell Dev Biol* 2011; **27**: 107–132.
44 Codogno P, Mehrpour M, Proikas-Cezanne T. Canonical and non-canonical autophagy: variations on a common theme of self-eating? *Nat Rev Mol Cell Biol* 2011; **13**: 7–12.
45 Terasawa K, Yoshimatsu K, Iemura SI, Natsume T, Tanaka K, Minami Y. Cdc37 interacts with the glycine-rich loop of Hsp90 client kinases. *Mol Cell Biol* 2006; **26**: 3378–3389.
46 Calderwood SK, Khaleque MA, Sawyer DB, Ciocca DR. Heat shock proteins in cancer: chaperones of tumorigenesis. *Trends Biochem Sci* 2006; **31**: 164–172.
47 Caplan AJ, Mandal AK, Theodoraki MA. Molecular chaperones and protein kinase quality control. *Trends Cell Biol* 2007; **17**: 87–92.
48 Jin DY, Spencer F, Jeang KT. Human T cell leukemia virus type 1 oncoprotein Tax targets the human mitotic checkpoint protein MAD1. *Cell* 1998; **93**: 81–91.
49 Giam CZ, Jeang KT. HTLV-1 Tax and adult T-cell leukemia. *Front Biosci* 2007; **12**: 1496–1507.
50 Tanaka Y. Activation of leukocyte function-associated antigen-1 on adult T-cell leukemia cells. *Leuk Lymphoma* 1999; **36**: 15–23.
51 Kawaguchi A, Orba Y, Kimura T, Iha H, Ogata M, Tsuji T *et al.* Inhibition of the SDF-1alpha-CXCR4 axis by the CXCR4 antagonist AMD3100 suppresses the migration of cultured cells from ATL patients and murine lymphoblastoid cells from HTLV-I Tax transgenic mice. *Blood* 2009; **114**: 2961–2968.
52 Hertlein E, Wagner AJ, Jones J, Lin TS, Maddocks KJ, Towns III WH *et al.* 17-DMAG targets the nuclear factor-kappaB family of proteins to induce apoptosis in chronic lymphocytic leukemia: clinical implications of HSP90 inhibition. *Blood* 2010; **116**: 45–53.
53 Yamamoto K, Utsunomiya A, Tobinai K, Tsukasaki K, Uike N, Uozumi K *et al.* Phase I study of KW-0761, a defucosylated humanized anti-CCR4 antibody, in relapsed patients with adult T-cell leukemia–lymphoma and peripheral T-cell lymphoma. *J Clin Oncol* 2010; **28**: 1591–1598.

Supplementary Information accompanies this paper on the Blood Cancer Journal website (http://www.nature.com/bcj).

Virology 443 (2013) 226–235

Contents lists available at SciVerse ScienceDirect

Virology

journal homepage: www.elsevier.com/locate/yviro

Failure in activation of the canonical NF-κB pathway by human T-cell leukemia virus type 1 Tax in non-hematopoietic cell lines

Terumi Mizukoshi [a], Hideyuki Komori [a,1], Mariko Mizuguchi [a], Hussein Abdelaziz [a,b], Toshifumi Hara [a,2], Masaya Higuchi [c], Yuetsu Tanaka [d], Yoshiro Ohara [e], Noriko Funato [a], Masahiro Fujii [c], Masataka Nakamura [a,*]

[a] Human Gene Sciences Center, Tokyo Medical and Dental University, 1-5-45 Yushima, Bunkyo-ku, Tokyo 113-8510, Japan
[b] Department of Medical Biochemistry, Faculty of Medicine, Mansoura University, Mansoura, Egypt
[c] Division of Virology, Niigata University Graduate School of Medical and Dental Sciences, Niigata, Japan
[d] Department of Immunology, Graduate School and Faculty of Medicine, Ryukyu University, Okinawa, Japan
[e] Department of Microbiology, Kanazawa Medical University, Ishikawa, Japan

ARTICLE INFO

Article history:
Received 21 January 2013
Returned to author for revisions
25 February 2013
Accepted 29 April 2013
Available online 18 June 2013

Keywords:
HTLV-1
Tax1
NF-κB
Canonical pathway
Transcription
Hematopoietic cells

ABSTRACT

Human T-cell leukemia virus type 1 (HTLV-1) Tax (Tax1) plays crucial roles in leukemogenesis in part through activation of NF-κB. In this study, we demonstrated that Tax1 activated an NF-κB binding (gpκB) site of the gp34/OX40 ligand gene in a cell type-dependent manner. Our examination showed that the gpκB site and authentic NF-κB (IgκB) site were activated by Tax1 in hematopoietic cell lines. Non-hematopoietic cell lines including hepatoma and fibroblast cell lines were not permissive to Tax1-mediated activation of the gpκB site, while the IgκB site was activated in those cells in association with binding of RelB. However RelA binding was not observed in the gpκB and IgκB sites. Our results suggest that HTLV-1 Tax1 fails to activate the canonical pathway of NF-κB in non-hematopoietic cell lines. Cell type-dependent activation of NF-κB by Tax1 could be associated with pathogenesis by HTLV-1 infection.

Introduction

Infection with human T-cell leukemia virus type1 (HTLV-1) causes adult T-cell leukemia (ATL) and inflammatory disorders such as HTLV-1 associated myelopathy/tropical spastic paraparesis and HTLV-1 associated uveitis (Hinuma et al., 1981; Osame et al., 1986; Poiesz et al., 1980). HTLV-1 encodes Tax1, which has been shown to be implicated in the pathogenesis of HTLV-1 associated disorders (Giam and Jeang, 2007). Tax1 is a trans-acting transcriptional regulator that exerts its function via cellular transcription factors mainly cAMP responsive element binding protein (CREB), nuclear factor κB (NF-κB) and serum responsive factor (SRF) (Ballard et al., 1988; Fujii et al., 1992; Lenzmeier et al., 1998). Tax1 interaction with cellular transcription factors leads to transcriptional changes in many cellular genes as well as activation of HTLV-1 transcription (Lenzmeier et al., 1998; Ohtani and Nakamura, 2002; Yoshida M., 2001; Zhao and Giam, 1992). Previous studies demonstrated that activation of NF-κB by Tax1 is closely associated with development and maintenance of ATL (Akagi et al., 1995; Ben-Neriah and Karin, 2011; Matsuoka and Jeang, 2007; Qu and Xiao, 2011). Tax1 activates both the NF-κB canonical and non-canonical pathways consisting of RelA with p50 and RelB with p52, respectively (Harhaj and Harhaj, 2005; Xiao et al., 2001). Activation of the canonical pathway results mainly from association of Tax1 with the IKK complex, leading to inactivation of IκB by phosphorylation, followed by translocation of the RelA/p50 complex to the nucleus (Geleziunas et al., 1998; Jin et al., 1999). Tax1 is also able to directly facilitate the transition of the precursor p100 into p52, thus promoting translocation of the non-canonical pathway complex RelB with p52 to the nucleus (Higuchi et al., 2007; Shoji et al., 2009). In the nucleus, NF-κB binds promoter DNA elements to initiate or enhance transcription of respective genes. The other member of the HTLV family is HTLV-2, which also produces a trans-acting transcriptional molecule so-called Tax2 (Ross et al., 1996). Tax2 does resemble Tax1 in terms of the ability to activate NF-κB and differs from Tax1 in that Tax2 predominantly activates the canonical NF-κB pathway (Higuchi et al., 2007; Shoji et al., 2009).

The gp34 gene was first identified to be a target of Tax1 in human T cells (Miura et al., 1991; Tanaka et al., 1985). Since its discovery, the gene product has been revealed as an OX40 ligand (OX40L), a type II transmembrane member of the tumor necrosis factor (TNF) superfamily, which is expressed on antigen presenting

* Corresponding author. Fax: +81 3 5803 0234.
E-mail address: naka.gene@tmd.ac.jp (M. Nakamura).
[1] Present address: Life Science Institute, University of Michigan, Ann Arbor, MI, USA.
[2] Present address: Genetics Branch, National Cancer Institute, National Institutes of Health, Bethesda, MD, USA.

0042-6822/$ - see front matter © 2013 Elsevier Inc. All rights reserved.
http://dx.doi.org/10.1016/j.virol.2013.04.032

cells, endothelial cells and activated T cells under normal immune conditions (Baum et al., 1994). OX40L interacts with OX40, a member of the TNF receptor family, which is predominantly expressed in T cell and delivers co-stimulatory signals implicated in expansion, survival and homeostasis of T cells (Ishii et al., 2010). Among ATL cells and HTLV-1 infected T cells, only T cells expressing Tax1 express OX40L on their cell surface. We previously reported that the gp34 (OX40L) gene promoter has an element capable of NF-κB binding (Ohtani et al., 1998). The NF-κB binding (gpκB) site is, at least in part, responsible for Tax1-mediated expression of OX40L on T cells. This Tax1-mediated expression makes the interaction of OX40 with OX40L possible in the same T cells. OX40 and OX40L interaction in ATL development remains to be examined. Our preliminary results indicate that the gpκB site in the OX40L promoter is somewhat different from the classical NF-κB binding site represented by the NF-κB binding site (Igκ B site) of the immunoglobulin light chain gene promoter. The gpκB site in the OX40L promoter fails to be activated in the presence of Tax1 in the fibroblast cell line REF52, in contrast to activation in the T cell line Jurkat.

In this study, we wished to understand how Tax1 activated the gpκB site in a cell type-dependent manner. Our results indicate that Tax1 does not activate the canonical NF-κB pathway in non-hematopoietic cell lines, suggesting involvement of Tax1 in T cell pathogenesis.

Results

Tax1 does not activate the gpκB site in non-hematopoietic cells

Tax1 activated the Igκ B and gpκB sites in Jurkat cells (Fig. 1), as shown previously (Ohtani et al., 1998). Unexpectedly, in REF52 cells, Tax1 did not activate the gpκB site, while the Igκ B site was activated (Fig. 1). We hypothesized that responses of the gpκB site to Tax1 might be cell lineage-dependent. To test this notion, more cell lines of hematopoietic and non-hematopoietic lineages were used for reporter assays with Tax1. Non-hematopoietic cell lines, the human osteosarcoma cell line MG63, the human hepatoma cell lines Huh7 and HepG2, the human cervical cancer cell line HeLa, the human embryonic kidney cell line 293T and the murine neuroblastoma cell line C-1300 exhibited Tax1-mediated activation of the Igκ B site, but the gpκB site was not activated in response to Tax1 in those cell lines (Fig. 1). A slight but not significant activation of the gpκB site by Tax1 was observed in HeLa and 293T cells, however this activation may be due to indirect effects of Tax1 (discussed later). Hematopoietic cell lines, the human Burkitt's lymphoma cell line Raji and the human myelogenous leukemia cell line K562, allowed activation of the gpκB site by Tax1 similar to Jurkat (Fig. 1). These results suggest that Tax1 does not activate the gpκB site in non-hematopoietic lineage cell lines.

In order to study cell type-dependent activation of the gpκB site by Tax1, we examined effects of ectopic expression of NF-κB subunits (RelA, p105/p50, RelB, p100/p52 and c-Rel) on the activation of the gpκB site in non-hematopoietic cell lines. The gpκB site was activated by overexpression of either RelA or p50 without Tax1 in REF52, MG63 and HeLa cells (Fig. 2A). Similarly RelA-dependent activation was seen with the Igκ B site (Fig. 2A). Increased activation by RelA was dose-dependent (Fig. S1). Ectopic expression of c-Rel slightly activated the gpκB site (Fig. 2A). Introduction of RelB or p52 combination however did not change reporter gene expression from the gpκB site, while the Igκ B site was activated by treatment with RelB (Fig. 2A and B). These results suggest that the canonical pathway is closely associated with activation of the gpκB sites in non-hematopoietic cells.

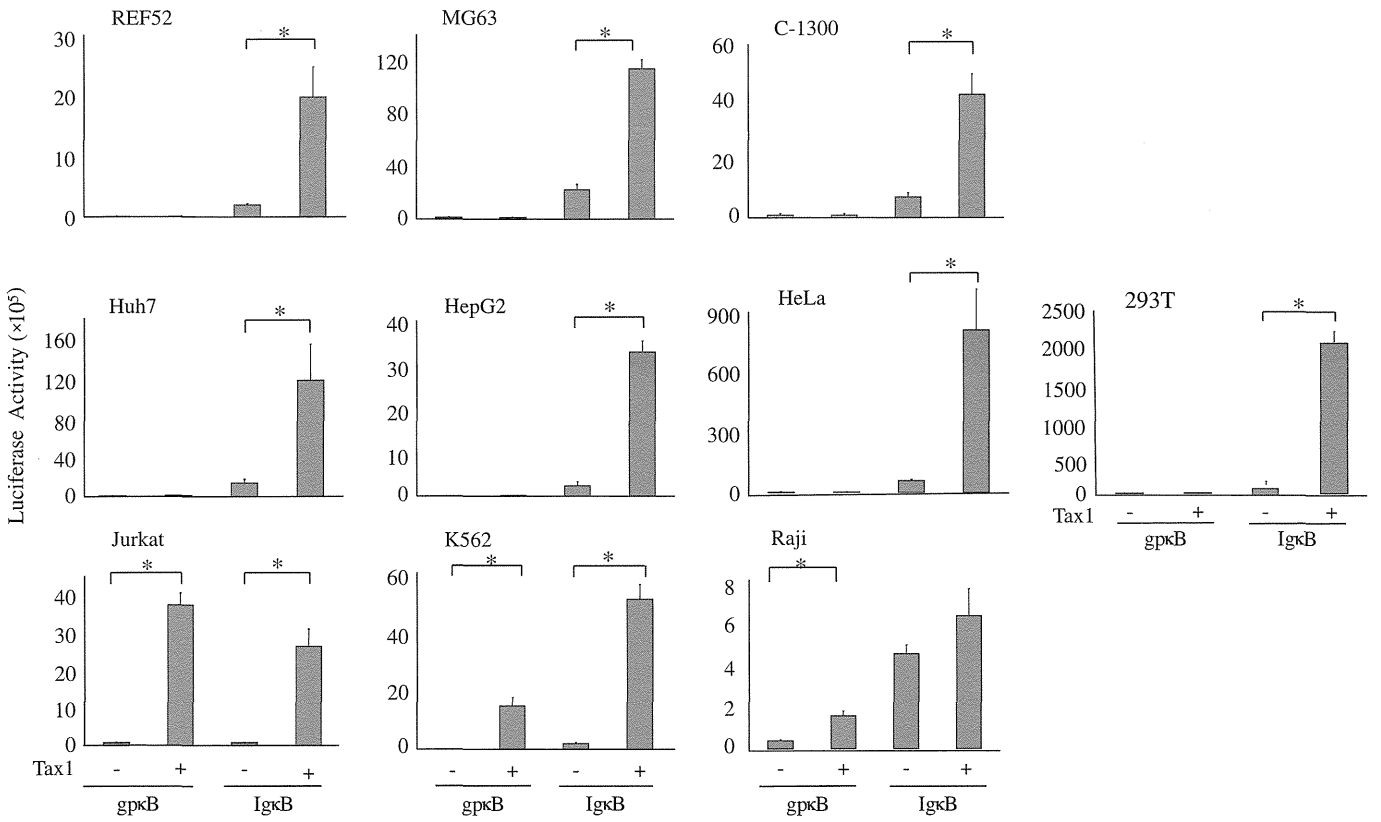

Fig. 1. Cell type-dependent activation of the gpκB site by Tax1. Cells were transfected with the gpκB or Igκ B reporter plasmid along with pMT-2Tax. REF52, MG63, HeLa, 293T, Jurkat, K562 and Raji cells were cultured for 48 h. Huh7, HepG2 and C-1300 cells were cultured for 24 h and harvested for luciferase activity determination. Luciferase activity was normalized to protein content. Data are means ± SE. $^{*}P < 0.05$.

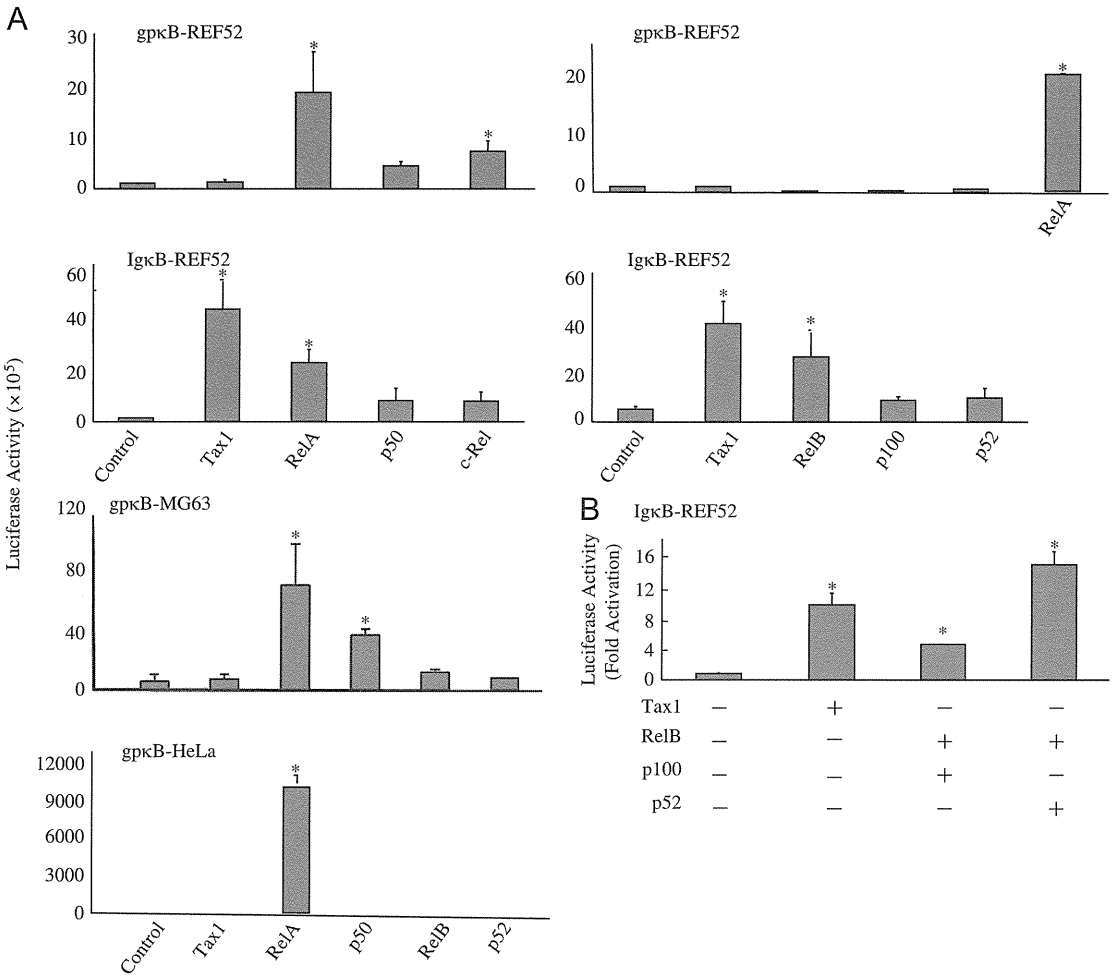

Fig. 2. Effects of NF-κB subunits on gpκB site activation. Expression plasmids for NF-κB subunits or Tax1 were transfected to REF52, HeLa and 293T cells along with the gpκB or IgκB reporter plasmid. Cells were cultured for 48 h and harvested for luciferase activity determination. Luciferase activity was normalized to protein content (A) or to β-galactosidase activity (B). Data are means ± SE. $^{*}P < 0.05$.

Tax1 activates the non-canonical NF-κB pathway in REF52 cells

Based on these results, we assumed the possibility that Tax1 did not activate the canonical pathway in non-hematopoietic cell lines and that the non-canonical pathway might be responsible for Tax1-dependent activation of the IgκB site. The assumption was examined by experiments with REF52 cells overexpressing the NF-κB subunits. Interestingly, overexpression of the non-canonical pathway subunit RelB alone or along with p52, a partner in the non-canonical pathway, significantly activated the IgκB sites in REF52 cells in the absence of Tax1 (Fig. 2A and B). Consistent with this, disruption of RelB or p52 by introduction of respective siRNA significantly reduced activation of the IgκB site by Tax1, while siRNA for RelA or p50 did not show appreciable effect (Fig. 3).

HTLV-2, a human retrovirus close to HTLV-1, produces Tax2, which is known to predominantly activate the canonical NF-κB pathway (Matsumoto et al., 1997). Similar to Tax1, Tax2 activated both gpκB and IgκB sites in Jurkat cells, while, in REF52 cells, the gpκB site was not activated by Tax2 (Fig. 4A). Tax2 exhibited significantly lower activation of the IgκB sites than Tax1 in REF52 cells (Fig. 4B). A chimera Tax mutant (Tax1/2) between Tax1 and Tax2, in which the Tax1 (225–232) region responsible for activation of the non-canonical pathway was replaced with a region of Tax2 (225–232), has little ability to activate the non-canonical pathway (Shoji et al., 2009). The effects of the Tax1/2 mutant on activation of the gpκB and IgκB sites were close to those of Tax2, rather than Tax1, in Jurkat and REF52 cells (Fig. 4). These results strongly indicate the possibilities that the gpκB site is activated by the canonical, but not non-canonical, pathway and that the canonical pathway is scarcely activated by Tax1 in non-hematopoietic cell lines.

RelA and p50 are expressed in non-hematoietic cells

We therefore examined expression and localization of NF-κB subunits in non-hematopoietic cells. Immunostaining and Western blot analyses clearly showed that REF52, MG63 and HeLa cells expressed RelA, p50, RelB and p52 (Fig. 5A–H). RelA was mainly present in the cytoplasm, while p50 was in the nucleus and cytoplasm (Fig. 5A–D). The ability of those subunits to bind κB sites was examined by electrophoreitic mobility shift assay (EMSA). In contrast to the cytoplasmic extracts which gave supershift bands with anti-RelA antibody, nuclear extracts from REF52 cells with or without Tax1 expression did not form complexes containing RelA with the gpκB site and the IgκB site (Fig. 6A and B). Binding of p50 was seen with both nuclear and cytoplasmic extracts; nuclear extracts from Tax1-expressing REF52 cells formed the most abundant complex. Ectopic expression of RelA in REF52 cells induced its complex formation with the gpκB site (Fig. 6C). Complexes containing RelA were also detected using nuclear extracts from REF52 cells ectopically expressing p50. These results are consistent with reporter assays. RelB, p52 and c-Rel were not included in complexes